A 21 CM SURVEY OF THE SOUTHERN MILKY WAY

By F. J. Kerr,* J. V. Hindman,* and C. S. Gum*

[*Manuscript received May 25, 1959*]

Summary

A study has been made of 21 cm hydrogen-line radiation around the Southern Milky Way, using a beamwidth of 1°·4 and a bandwidth of 40 kc/s (8·5 km/sec).

The surveyed strip of sky was sampled by recording the intensity of the radiation along 41 discrete tracks across the galactic equator, in the longitude range 175°–5° ("old" system of coordinates). The tracks were generally spaced 5° apart in longitude, and were in most cases along lines of constant declination. The range of galactic latitude of the tracks varied from 9° to 1°·5, for reasons connected with the programming of the survey.

The observations were taken on a four-channel statically balanced receiver; one run along a track yielded the variation of intensity as a continuous function of sky position at four fixed frequencies. Records were taken at a sufficient number of discrete frequencies to cover the full frequency range of the line.

The results are presented in the form of contour diagrams showing the 21 cm intensity along each track as a function of latitude and radial velocity. In addition, line profiles are given for a series of points around the "new" galactic equator.

A combination of this survey and that carried out for the northern sky by the Leiden group gives a coverage of the whole galactic circle at approximately the same resolution. There is good agreement between the two sets of results in the common range of longitude.

I. Introduction

Observations of the 21 cm line from interstellar atomic hydrogen provide the best of the known methods for investigating the large-scale structure of the Galaxy. Not only is radiation detectable from substantially the whole Galaxy but contributions from different distances can generally be distinguished, through the Doppler dispersion produced by galactic rotation effects. By contrast, optical studies are restricted to the solar neighbourhood, while radio continuum observations can only provide an integrated intensity along each line of sight.

The first survey of 21 cm radiation over a substantial part of the sky was carried out in Sydney by Christiansen and Hindman (1952), soon after the initial detection of the line by Ewen and Purcell (1951). This early survey showed the high degree of concentration towards the galactic plane, and gave the first 21 cm indication of spiral arms. The strip of sky in the vicinity of the galactic equator has special interest for studies of large-scale galactic structure. An extensive investigation of the northern part of this strip has been carried out by the Leiden group (van de Hulst, Muller, and Oort 1954; Muller and Westerhout 1957) and this has led to a picture of the spiral structure of the Galaxy over the range of longitude accessible from Holland (Schmidt 1957; Westerhout 1957).

* Division of Radiophysics, C.S.I.R.O., University Grounds, Chippendale, N.S.W.

The outstanding uncertainty in deriving the three-dimensional distribution of galactic hydrogen from 21 cm observations is the choice of a rotational velocity model for relating Doppler shifts and distance. Observations from a southern hemisphere observatory, besides being important in themselves for completing a galactic survey, are essential for a test of the assumptions made in interpreting the observations, and particularly of the rotation model adopted.

The present paper gives the results of a survey covering the southern part of the Milky Way strip, using a beamwidth of 1°·4 and a bandwidth equivalent to 8·5 km/sec. In order to study the thin layer of hydrogen, observations were taken along 41 " tracks " crossing the galactic equator in the longitude range 175°–5° (" old " system of coordinates). In most cases these tracks were lines of constant declination, the observations being made with a stationary aerial; the frequency of the receiver always remained constant during an observation. Four separate channels were used, providing simultaneous records in four adjacent 40 kc/s bands, which could be set to any desired position in the frequency range of the line.

This method of observation was chosen because the aerial was limited to meridian operation. The combination of transit aerial and fixed-frequency receiver was very suitable for obtaining the variation of intensity across the sky, for example, in locating the galactic plane. On the other hand, line profiles had to be derived from a series of observations along each track at a number of discrete frequencies.

The results of the survey are presented in the form of contour diagrams, each showing the variation of brightness temperature as a function of galactic latitude and radial velocity for a particular track. Line profiles may be derived from diagrams of this type by taking horizontal sections. A set of profiles for points on the new galactic equator has also been included in the paper; such profiles are the most significant for galactic structure studies and they also provide a quick assessment of the variation with longitude.

This paper is appearing during the transition period when the " old " system of galactic coordinates (Ohlsson 1932) is being superseded by a " new " system (Blaauw *et al.* 1959). The results are presented primarily in terms of the old coordinates, as the survey was carried out in terms of that system, but the new coordinates are also given in the diagrams as far as possible. The symbols l^{I}, b^{I} are used throughout for the old coordinates and l^{II}, b^{II} for the new.

Taken together, the Leiden and Sydney surveys cover the full 360° range of galactic longitude, at approximately the same resolution in angle and velocity. There is sufficient overlap in longitude to permit a good check of the homogeneity of the combined data.

A progress report on the analysis of the southern survey has been given by Kerr, Hindman, and Carpenter (1957), and the results have also been used by Oort, Kerr, and Westerhout (1958) in a first discussion of the combined Leiden and Sydney data. In addition, IAU Subcommission 33b has taken into account the new information on the shape of the hydrogen layer in its revision of the system of galactic coordinates (Gum and Kerr 1958; Gum and Pawsey 1958; Blaauw *et al.* 1959). The present paper gives the observational results only; these results will be discussed in later papers.

II. Aerial

The observations were taken with the Radiophysics Laboratory's 36 ft. paraboloid, which is mounted on an east-west axis as a transit instrument.* The aerial is located at Potts Hill, near Sydney, at latitude $33°\cdot 9$ S. and longitude $151°\cdot 0$ E.

The aerial is fed by a flanged horn, carried on a four-legged support attached to the rim of the dish, and both the waveguide crystal mixer and the intermediate-frequency pre-amplifier are located near the feed point. The polarization of the electric vector is horizontal, i.e. parallel to the east-west axis.

(*a*) *Beam Characteristics*

The directional diagram was derived with the Sun as a source by sweeping in declination during the period of a solar transit; allowance was made for the finite diameter of the solar disk. Check measurements were made on several discrete sources of cosmic noise, but these were less accurate owing to the lower intensity.

The main beam was found to be nearly Gaussian, with a half-power width of $1°\cdot 4$ and an approximately circular cross section. The near side lobes were 23 dB below the peak intensity.

To derive the brightness temperature in the sky from measured values of aerial temperature, we must determine the *net efficiency*† of the aerial. This may be defined as that fraction of the total input power which would go into the main lobe if the aerial were used to transmit instead of receive. It takes account of losses in the system, and also discriminates between the radiation in the main beam and its adjoining side lobes and that in the "stray" field, the remainder of the sphere.

The gain of the aerial was measured by a comparison with a known horn, using the Sun as a reference source. The gain was found to be $41\cdot 8 \pm 0\cdot 3$ dB, leading to a value for the *aperture efficiency* of the paraboloid (the ratio of the effective area to the geometrical area) of $0\cdot 56 \pm 0\cdot 05$. The *net efficiency* was then derived by integrating over the full beam, with the absolute level fixed by the gain measurement. The value obtained was $0\cdot 78$.

(*b*) *Position Measurement*

The primary position calibration was carried out on the strong radiation from the Sun over the range of declination covered by the ecliptic. By moving the aerial in small steps during a solar transit, calibration points in declination were obtained with an accuracy of $\pm 0°\cdot 03$. The calibration was extended

* A photograph of the aerial has been published by Kerr, Hindman, and Robinson (1954).

† This quantity is related to, but differs from, the "diffractive efficiency" defined by Seeger, Westerhout, and van de Hulst (1956) (Wade, in preparation). It must be multiplied by a factor which depends on the angular extent of the source, if the source covers an appreciable fraction of the whole sky.

over the rest of the declination range by visual sights across the face of the dish during the transit of stars. These visual checks depended on the assumption that the dish and feed structures moved as a single unit when the declination was changed. This assumption is known to be valid over the Sun's range of declination, but cannot be tested so precisely outside this range. An additional check was provided by a position measurement on the source Centaurus A (Hindman and Wade 1959).

Scale errors of a few tenths of a degree were found to occur in some parts of the declination range, arising from distortion of the structure which supports the dish. These errors were closely reproducible and were satisfactorily allowed for through a calibration table. Periodical checks were made on the Sun to ensure that the scale zeros had not moved significantly, and the whole process of Sun and star checks was carried out on three separate occasions.

Table 1

COMPARISON BETWEEN SYDNEY AND LEIDEN AERIAL SCALES THROUGH MEASUREMENTS ON THE SOURCE SGR A

Aerial	Beamwidth	Right Ascension (1950)	Declination (1950)	Reference
Sydney, Potts Hill	$1°\cdot4$	$17^h\ 42^m\cdot7\pm0^m\cdot2$	$-29°\ 01'\pm5'$	
Leiden, Kootwijk	$1°\cdot8$ by $2°\cdot8$			
1954 ..		$17^h\ 42^m\cdot0\pm0^m\cdot8$	$-28°\ 58'\pm15'$	Westerhout (personal communication)
1955 ..		$17^h\ 42^m\cdot1\pm0^m\cdot8$	$-29°\ 02'\pm15'$	
IAU Comm. 33b mean	—	$17^h\ 42^m\cdot6\pm0^m\cdot06$	$-28°\ 57'\pm1'$	Gum and Pawsey (personal communication)

The Right Ascension calibration was based on the same radio and visual observations. The alignment of the radio axis with the meridian was checked in this way to an accuracy of $\pm0°\cdot02$. In addition, allowance had to be made for the time delay in the receiver, which produced an apparent shift of Right Ascension on a constant declination track. Other factors which affect the accuracy of the position measurements are: rounding-off errors in setting the scale (in the case of declination), errors in reading time from the records (in the case of Right Ascension), and, finally, the slight errors introduced in the conversion from equatorial to galactic coordinates. The overall uncertainty of the position measurements in the survey is estimated to be $\pm0°\cdot07$ in each galactic coordinate.

A combination of the Sydney and Leiden surveys is necessary to give an overall picture of the whole Galaxy; consequently, some direct comparisons have been made to guard against the possibility of systematic position errors in either set of data. The most precise of these comparisons was made through the discrete source Sagittarius A (IAU 17S2A), with the results shown in Table 1. The Leiden survey was carried out with the Kootwijk aerial. For comparison, the table includes a recent mean position derived by IAU Subcommission 33b from measurements made with the larger reflectors at Dwingeloo, Stockert, and Washington (Blaauw *et al.* 1959). The Sydney and Kootwijk values agree with one another and with the more accurate position to well within their probable errors.

III. Receiver

(*a*) *Description of Receiver*

The receiver used in the survey departed from the usual practice of switching between two frequencies, one of which is on the line and the other away from it. Instead, the difference in the receiver output at the two frequencies was measured continuously by connecting the two channels to opposite sides of a differential D.C. amplifier. The front portion of the receiver followed conventional practice, with intermediate frequencies at 30 and 7 Mc/s. A block diagram of the later sections is shown in Figure 1.

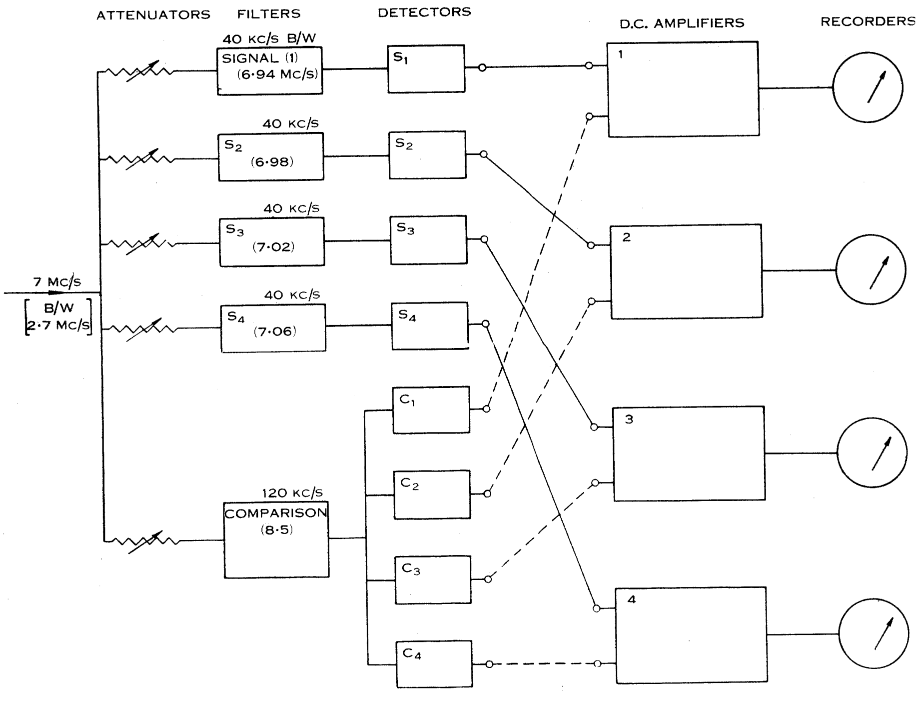

Fig. 1.—Block diagram of later sections of receiver.

The receiver noise factor, measured with a continuous-spectrum source, varied between 6 and 8 dB during the period of the survey. The effective noise factor for the detection of line radiation was about 3 dB higher, since the contributions of receiver noise at the signal and image frequencies were approximately equal.

The first local oscillator, at 1390 Mc/s, was variable in frequency, so that the block of signal channels could be moved across a line profile; a temperature-controlled oscillator, operating at about 5·7 Mc/s, was followed by five tripling stages. The second local oscillator was a self-excited oscillator at 37 Mc/s.

The main i.f. amplifiers, whose overall bandwidth was $2 \cdot 7$ Mc/s, were followed by a system of passive filters which selected specific portions of this pass band. Four of these filters were used as signal channels to receive the line; their half-power bandwidth was 40 kc/s and they were spaced about 40 kc/s apart. Single-tuned circuits were used in the filters; 90 per cent. of the noise response was within a band of 70 kc/s. A fifth filter, placed $1 \cdot 6$ Mc/s away from the signal filters, was used as the comparison channel. Its bandwidth was made somewhat larger (120 kc/s) to reduce the noise fluctuations in the receiver output. The levels in the various channels were controlled by attenuators at the output of the 7 Mc/s amplifier.

The outputs of the filters were fed to diode detectors which were linear to within 1 per cent. over the observed range of brightness temperatures. Four separate detectors were attached to the comparison filter to minimize interaction between the four channels.

Following the detectors, the difference voltage between each pair of signal and comparison channels was fed to an integrating circuit and a D.C. amplifier. The overall time delay of the whole receiver was measured on simulated galactic crossings which were produced by varying the output of an artificial signal source; a value of 25 sec was obtained.

The receiver was balanced with the aerial pointed towards a " cold " part of the sky. In any other direction, the output of the D.C. amplifier was then proportional to the amount of line radiation in the " signal " channel.

Most 21 cm line work to date has been done with receivers which are swept over the frequency range containing the line, and the levels on and off the line are compared by switching rapidly between the signal and comparison channels.

The statically balanced receiver avoids two of the major problems which must be overcome in stabilizing the switched and swept type of receiver. These are the maintenance of a flat base line while tuning over a wide frequency band and the precise equalizing of local oscillator output and front-end performance in the two switched positions. Instead of these, a new difficulty arises, owing to the fact that the signal and comparison channels use different parts of the i.f. pass band: the gain of the two channels can change differentially for quite small changes in the shape of the pass band.

In practice, the receiver proved difficult to stabilize, but close temperature control of the whole i.f. amplifier and the filter units and careful work on all critical parts of the system have brought the performance to a state where the base line follows a straight line to within ± 1 °K over a period of half an hour or so. During the period occupied by this survey, the receiver performance gradually improved but the observational data were all satisfactorily tied together.

The normal method used to establish the zero level was to make a measurement at the South Celestial Pole before and after each galactic crossing. This type of check is difficult if motion of the aerial itself produces a significant change in the receiver output level as the orientation of the pre-amplifier and other units varies. Such an effect was present during part of the survey, but it was monitored throughout the whole programme by checking the output level over a wide range of declination in the cold parts of the sky.

(*b*) *Temperature Calibration*

The absolute temperature scale of the receiver was calibrated by a two-step process : the noise factor of the receiver was first obtained and then a calibration of the D.C. amplifier was used to relate a change in aerial temperature to the corresponding change in the receiver output voltage. The noise factor was measured with the aid of a gas-discharge noise generator of waveguide type, connected to a horn which was placed immediately in front of the feed horn.

The overall result of these measurements showed that one recorder scale unit corresponded to $3 \cdot 2$ °K of aerial temperature when the receiver was operating in the condition which was adopted as the standard. The probable error of this absolute calibration is estimated to be about ± 15 per cent. ; relative checks of the day-to-day variations in sensitivity could, however, be made with an accuracy of ± 7 per cent., using the methods to be described in the next section.

The corresponding values of brightness temperature T_b are less certain ; the conversion from aerial temperature to brightness temperature is complex because the amount of galactic radiation picked up by the stray field varies as the aerial points to different directions in the sky. The net efficiency of the aerial, as described in Section II (*a*) above, was found to be $0 \cdot 78 \pm 0 \cdot 06$. Therefore, on the average,

$$T_b \approx 1 \cdot 28 T_a,$$

with the proportionality factor varying by a few per cent. from point to point in the sky.

(*c*) *Frequency Calibration*

The receiver was tuned by varying the first local oscillator. Measuring the operating frequency for each signal channel involved a measurement of its three components, the frequencies of the two local oscillators (1390 and 37 Mc/s) and the associated narrow-band filter (about 7 Mc/s). With an overall pass band of 40 kc/s, an accuracy of several kilocycles per second was required in each case ; thus only the first of the three measurements offered any difficulty.

The method adopted made use of a crystal-controlled oscillator (occasionally checked against WWVH) as a local reference standard for measuring the frequency of the $5 \cdot 7$ Mc/s oscillator. The beat note between the two oscillators, which was in the range from zero to 5000 c/s, was continuously monitored on a cathode-ray tube against a calibrated audio oscillator. The sign of the frequency difference was checked by producing a known frequency shift in the tunable oscillator. For convenience, the second local oscillator was adjusted so that zero beat was obtained when the receiver frequency corresponded to zero radial velocity ($1420 \cdot 405$ Mc/s). Then, for other settings of the receiver, the beat note was a direct measure of the radial velocity at which observations were being made. By this procedure, the receiver frequency could be measured to an accuracy of about $0 \cdot 5$ kc/s ($0 \cdot 1$ km/sec in velocity). In the later stages of the survey, the frequency was always stable to about one part in 10^6, i.e. $1 \cdot 5$ kc/s, over the period of a galactic crossing.

IV. Observing Programme

In this section we discuss the layout of the " tracks " which were used to sample the Southern Milky Way strip and the manner in which the observations were arranged in order to cover the full frequency range for each track.

(a) *Area Covered*

Observations have been taken over the whole stretch of the Milky Way which is accessible from Sydney, but the main attention has been concentrated on the southern part. The results presented in this paper cover the range of longitude from 175° to 5° (old system) ; this range provides a good overlap with

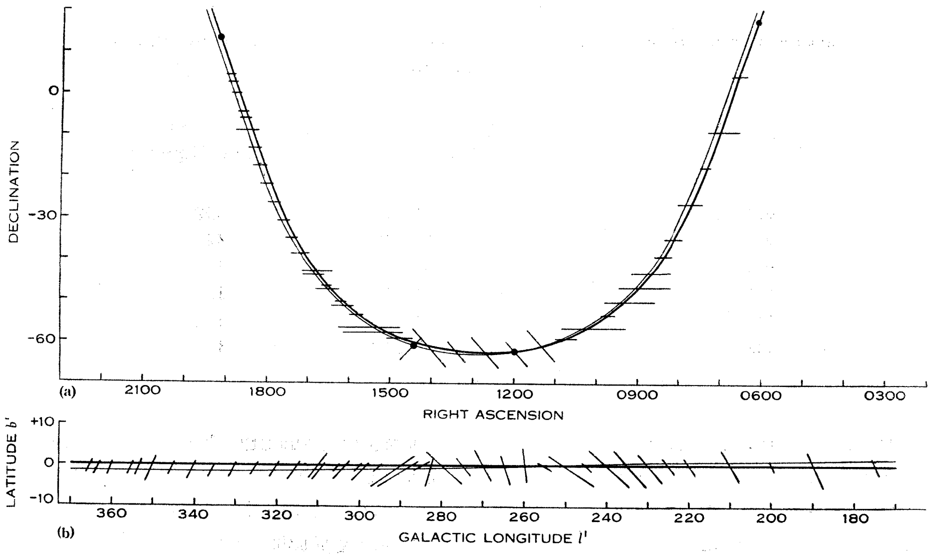

Fig. 2.—Layout of the 41 tracks along which observations were taken, showing also the old (——) and new (——) galactic equators. (*a*) Celestial coordinates (epoch 1955). The dots represent check points. (*b*) Old galactic coordinates.

the Leiden observations in the regions l^I=175°–220° and 320°–5°. A number of records have also been obtained in the rest of the accessible range (l^I=115°–175° and 5°–65°) ; these have been used in a study of the flatness of the hydrogen layer but have not otherwise been reduced.

(b) *Track System*

The surveyed area was sampled by taking observations along 41 tracks crossing the galactic equator. On each day of the programme, observations were made along a series of these tracks, with a check to the South Celestial Pole for a zero reference between successive tracks.

The layout of the track system on the sky is shown in Figure 2, in both celestial and (old) galactic coordinates. Most of the tracks were at constant declination, except in the southernmost region, where the latitude changes very slowly along a constant-declination line. In this section several special tracks were used, in which the declination was varied by the operator at a rate of 0°·2 per minute during the period of the observation. The declination values for the constant-declination tracks are given in the titles of the contour diagrams (Plates 1–41); the special tracks are defined in Table 2.

The galactic coordinates, in the old system, of any point on the tracks can be obtained from Figure 3. For many purposes, however, the tracks can be regarded as effectively normal to the galactic equator, because the intensity varies much more slowly with longitude than with latitude. For the remainder of the paper, the tracks are identified by the (old) longitude at which they cross the old galactic equator.

TABLE 2

SPECIFICATION OF THE VARIABLE-DECLINATION TRACKS IN THE SOUTHERN-MOST REGION

l^{I} at Old Equator	Declination (1955)	l^{II} at New Equator
260°·0	$-64°·8+0°·2\ (\alpha-11^{h}\ 00^{m})_{min.}$	292°·3
264°·8	$-64°·2+0°·2\ (\alpha-11^{h}\ 48^{m})$	297°·1
269°·9	$-66°·4+0°·2\ (\alpha-12^{h}\ 22^{m})$	302°·0
274°·8	$-64°·8+0°·2\ (\alpha-13^{h}\ 10^{m})$	306°·8
279°·8	$-66°·2+0°·2\ (\alpha-13^{h}\ 38^{m})$	311°·5
282°·7	$-58°·2-0°·2\ (\alpha-14^{h}\ 17^{m})$	315°·1

In the longitude range 220°–5°, there is a track crossing the galactic equator at least every 5°,* with some additional tracks in the range corresponding to the inner region of the Galaxy. These extra tracks were chosen to pass through points which were exactly symmetrical about the galactic centre with points on the main programme, in order to study the symmetry of the velocity pattern.

The latitude ranges of the individual tracks varied from 9° to 1°·5. The track lengths were chosen in such a way that a number of tracks could always be followed in each observing session. A few of the tracks were uncomfortably short, but most of the gas in the thin hydrogen layer is contained in the surveyed strip. In southern longitudes, the bulk of the gas that we are studying is at large distances and is therefore confined to a small latitude range. In general, the tracks were centred approximately on our first rough determination of a *new* galactic plane, but the shorter tracks were displaced, to meet the additional requirement that each track should include a point on the *old* galactic equator.

A sample record on the four-channel system is given in Figure 4. This contains a group of three tracks, at the longitudes marked in the figure, separated by short periods at the South Celestial Pole. (Other tracks in the same longitude range were covered in different series of observations.)

* Observations are now available at integral 5° intervals, right around the old galactic equator, from either the Leiden or Sydney survey.

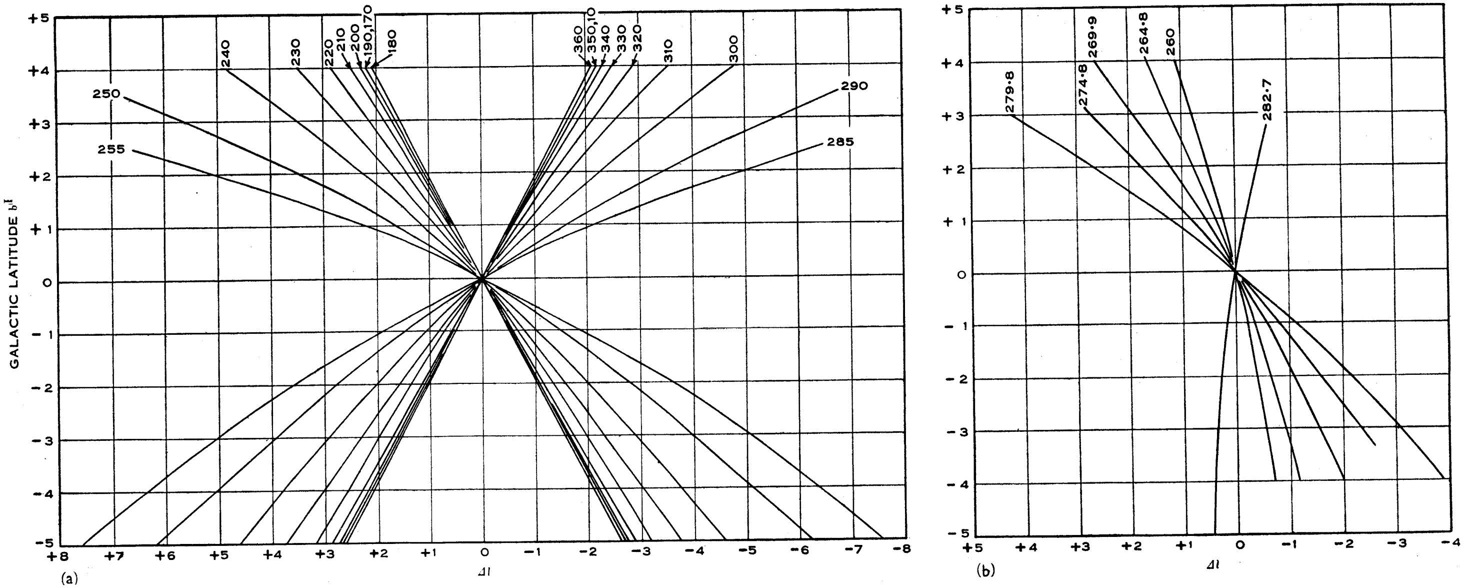

Fig. 3.—Galactic coordinates (old system) along the tracks. The abscissa is the difference between l^{I} at a point on the track and its value at the equator. The labels give the longitude at the equator. (*a*) Constant-declination tracks. Intermediate tracks can be found by interpolation. (*b*) Special manually operated tracks.

(c) *Frequency Coverage*

To cover the whole frequency range in which radiation could be detected, a number of runs were taken over each track with the four-channel block placed at a series of different frequencies. There was always an overlap of one channel width between successive runs and each frequency was used two or more times. In some cases, the frequency range was covered again at interlaced frequencies to give a half-channel spacing for the points.

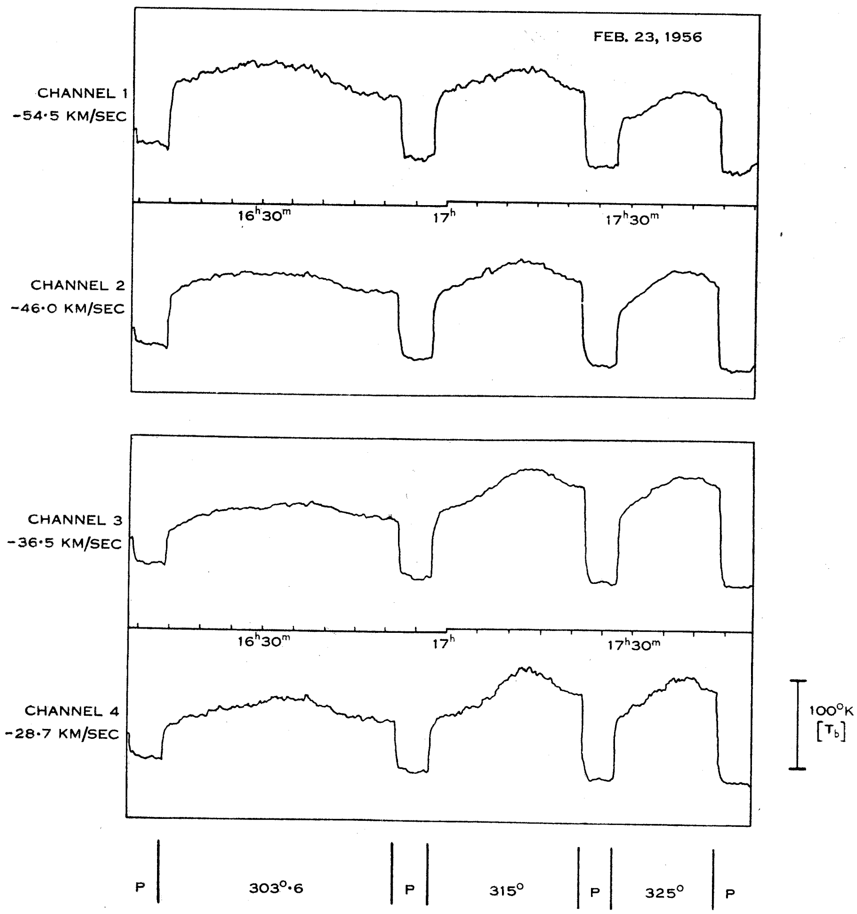

Fig. 4.—A sample four-channel record, consisting of fixed-frequency drift curves along three constant-declination tracks across the Galaxy, with check periods on the South Celestial Pole (*P*). The tracks are identified at the bottom of the diagram. (The radial velocities in this figure are the constant observational velocities, not corrected for local motions.)

A series of runs taken over a short period of time was always fairly uniformly spaced in frequency, the points being usually a channel width apart, but a repeat series taken at a later date would in general give runs at somewhat different frequencies, thus resulting in an irregular distribution of points along the line profile. The main reason for this difference was that, for convenience of operation, a succession of longitudes would be observed at the same actual frequency on a given day. The corrections to be applied for Sun and Earth motions had a different pattern at different times of year, with the result that the final corrected velocities at a given longitude show an uneven distribution.

The manner in which the points were distributed over the velocity range covered by the line is illustrated in Figure 6 below. Over the whole programme, there were an average of 6 runs per band width. The total number of galactic crossings in the whole project was about 6000, counting the records from the four channels separately.

(d) Calibration Checks

Three types of check were done at frequent intervals throughout the survey to monitor variations in the intensity scale. These comprised observations of low- and high-level standard regions in the sky, and checks of the gain of each of the four D.C. amplifiers.

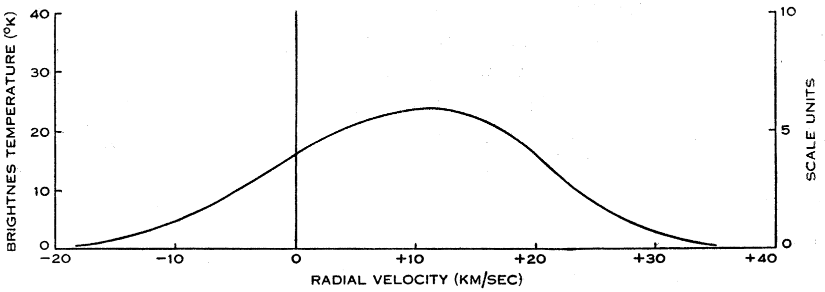

Fig. 5.—Line profile at the South Celestial Pole, the comparison point used for checking the receiver base line. (No radiation was detectable in the wings out to at least ± 200 km/sec.)

The South Celestial Pole was used for low-level checks, because it was always accessible, and the intensity there is effectively zero at most velocities. There is, however, a substantial level of radiation over a range of velocity near zero. The profile at the Pole therefore had to be determined and this was done by a careful series of comparisons with the regions of the two galactic poles. The real zero level of the survey at any particular velocity is therefore the mean level near the two galactic poles. This reference level is believed to be low, because there was no detectable variation over a large area of the sky and over the whole velocity range used in the survey; some broadly distributed radiation from the galactic halo or from beyond the Galaxy could still be present, however, as this would be difficult to detect.

The profile obtained at the celestial pole is shown in Figure 5. The nominal zero level had to be corrected for this radiation in all observations at low velocities.

For some of the runs at high radial velocities, where the galactic ridge is narrow and of low intensity, the zero level was taken from a long base line on either side of the galactic crossing, rather than from the South Pole. This method had the advantage that any effect arising from aerial movement was eliminated, but it could only be used for a small proportion of the runs, because of time limitations.

High-level check points were observed near the beginning, middle, and end of each day's programme. The positions of these standard regions are indicated in Figure 2. (The check points at 265° and 282° were alternatives.) Each of these points had to be observed at the same velocity (corrected for local motions) on each occasion, in order to obtain the standard check signal; therefore the receiver had to be retuned for a check point observation. South Pole observations, on the other hand, were always made at the frequency of the associated galactic crossing.

V. Method of Reduction

(*a*) *Frequency*

The frequency of the centre point of the four-channel block at which an observation was taken was first determined from measurements of the two local oscillator frequencies, and the corresponding radial velocity was then corrected for the Earth's velocity relative to the local centre of rest. The corrections for points on the old galactic equator were obtained from a set of tables kindly supplied by Leiden Observatory, which give the resultant of the velocities of the Earth and the Sun,* every 5° around the (old) galactic equator and every 5 days throughout the year. To obtain the velocities at points away from the equator, additional tables were prepared giving the velocity *gradient* along constant declination lines and the special tracks, as a function of date (Gill 1955).

Finally, the velocities corresponding to the four individual channels were derived from the corrected central velocity and the known frequencies of the four narrow-band filters.

(*b*) *Intensity*

For each galactic crossing, the intensity was read from the record at a series of times corresponding to integral half-degrees of latitude (b^{I}) along a smoothed line drawn through the noise fluctuations. The relative scale factor was corrected back to a standard condition, from the associated calibrations, and the zero level was found from the mean of the pole comparisons before and after the run, adjustments being made for any radiation at the pole at the frequency of observation. (A separate correction was needed for the component of the Sun and Earth motions, in the direction of the pole.)

(*c*) *Assembly of Crossings*

In reducing the set of galactic crossings for a particular track, the objective was to produce a " contour diagram " in which the intensity is plotted as a function of radial velocity and galactic latitude.

The first step was to plot out one profile (usually for $b^{\mathrm{I}}=0$), in order to check the agreement between the various observations. This profile check enabled any obviously deviant results to be found and rejected. The scatter of

* The solar motion was taken as 20·0 km/sec directed towards $\alpha=18^{\mathrm{h}}\,00^{\mathrm{m}}$, $\delta=+30°\cdot0$ (1900).

the individual points in a typical case can be seen in Figure 6. The r.m.s. deviation of the observed points from the corresponding mean profile, averaged over all the tracks, amounted to ± 2 °K in brightness temperature.

A diagram of this type was then used in grouping the observations at neighbouring velocities in order to form mean crossing-curves. The velocity spread inside a group was made large enough to contain a reasonable number of observations for averaging and small enough to avoid undue smoothing of the profile in the velocity direction. The velocity range covered by the points in a group averaged about 5 km/sec. Two sample comparisons between the various crossing-curves in a group are illustrated in Figure 7.

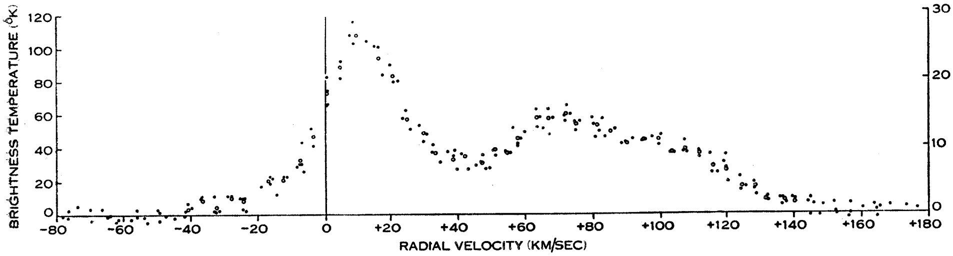

Fig. 6.—An illustration of the scatter of the points used to build up a profile ($l^{\mathrm{I}}=230°$, $b^{\mathrm{I}}=0°$). ● Individual points, ○ mean points.

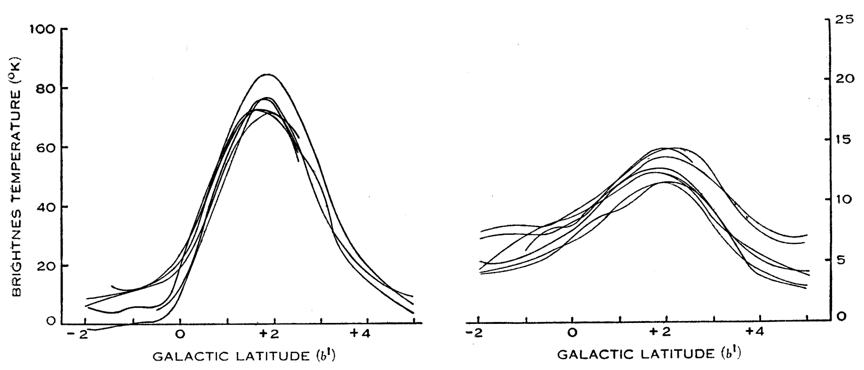

Fig. 7.—Two groups of galactic crossing-curves, illustrating the degree of reproducibility. 350° track. Velocity range: (*a*) $+101\cdot9$ to $+104\cdot2$ km/sec; (*b*) $-11\cdot1$ to $-6\cdot8$ km/sec.

A mean crossing-curve was prepared for each group by averaging the individual curves, and mean values were computed for the velocity at $b^{\mathrm{I}}=0$ and for the velocity gradient along the track. The latitude scale was corrected at this stage for the receiver time delay.

The latitudes at which each mean crossing-curve reached a set of fixed values were then read and plotted at the appropriate velocities on a velocity–latitude grid; contours were drawn through these points, with a small amount of additional smoothing.

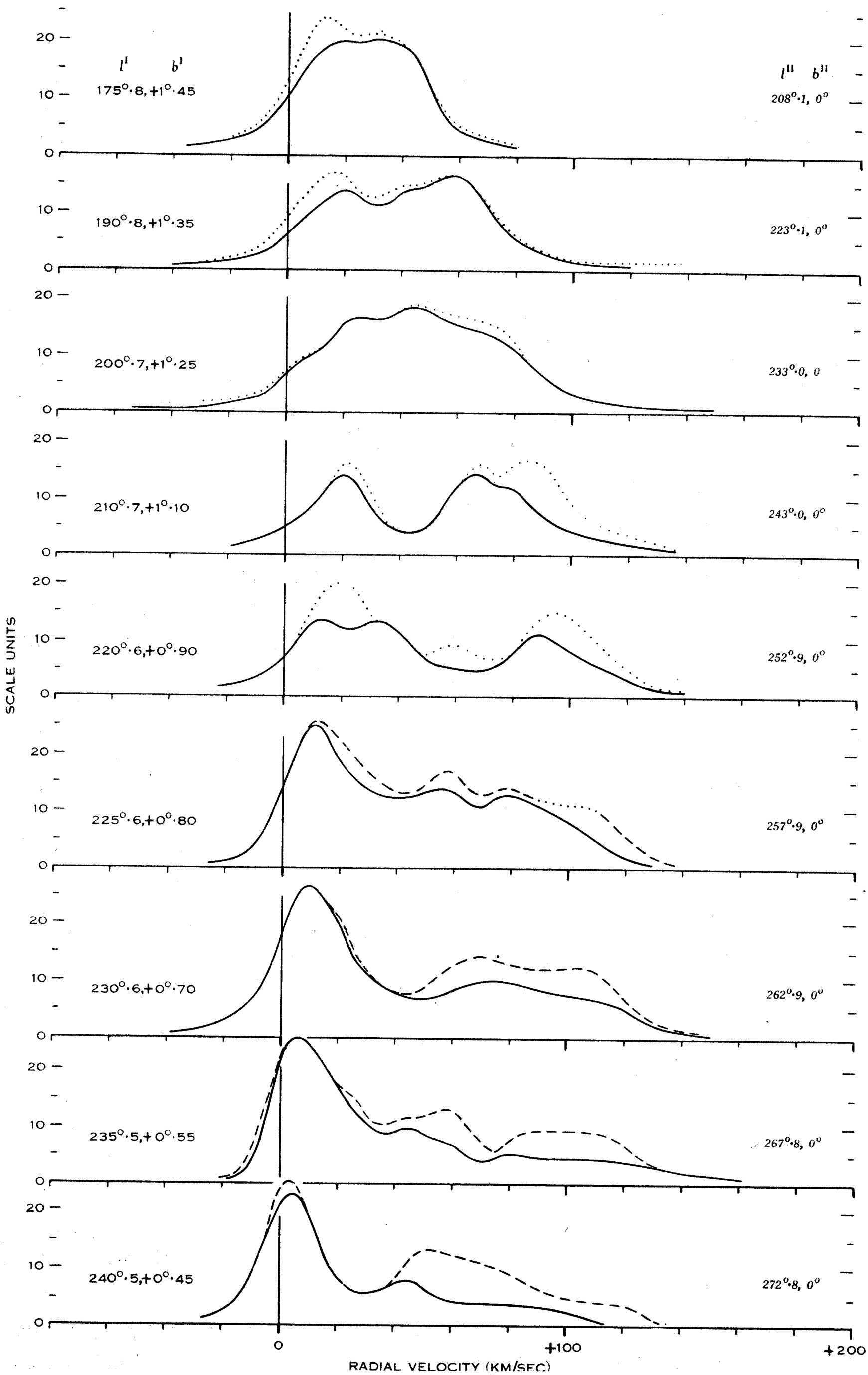

Fig. 8.—Profiles at new galactic equator ———— ; ridge-line profiles (see Section VI (*b*)) – – – – · · · ·. Unit = 3·2 °K in T_a, 4·1 °K in T_b.

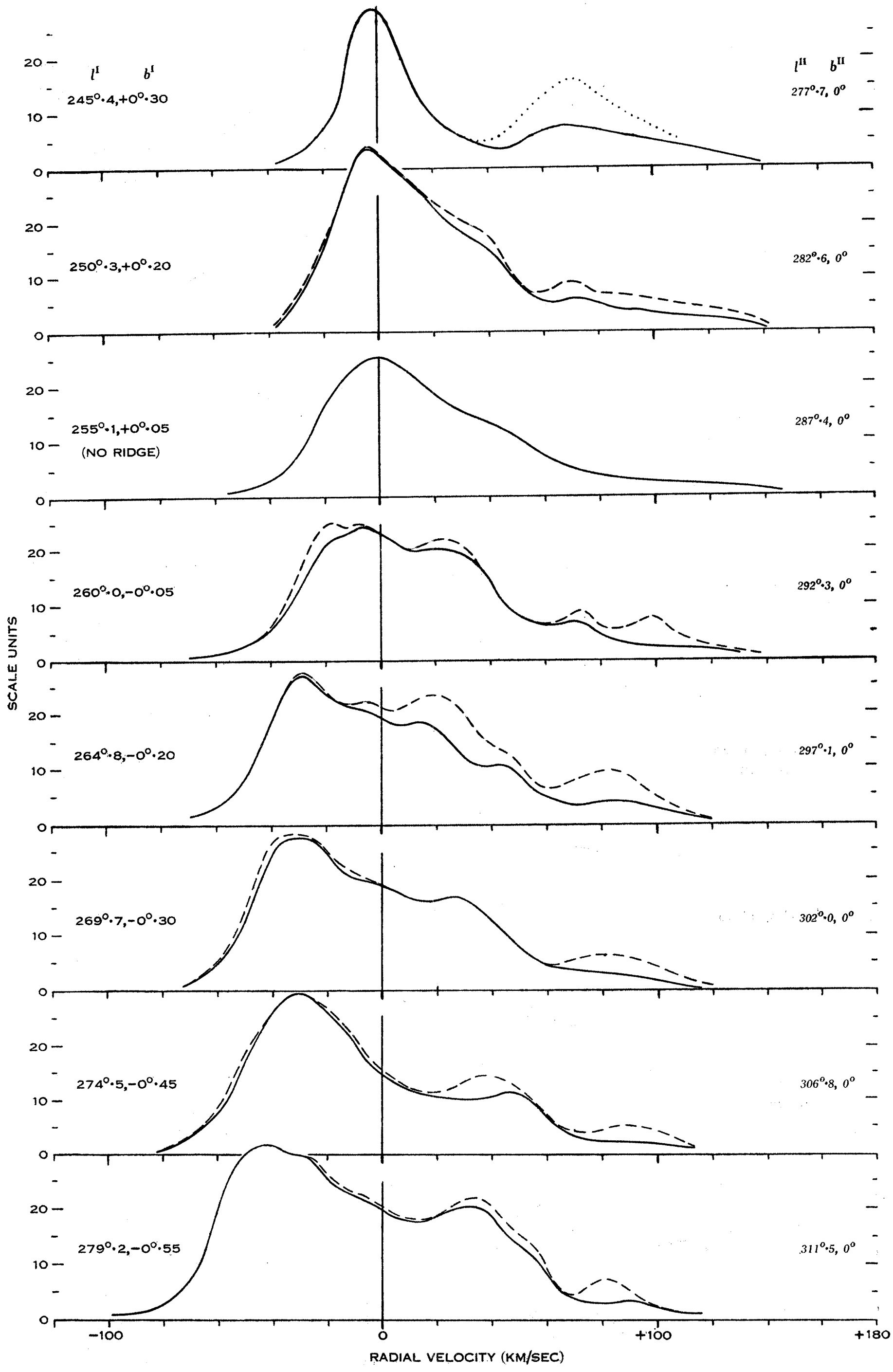

Fig. 9.—Profiles at new galactic equator ——— ; ridge-line profiles (see Section VI (*b*)) – – – ·····. Unit = 3·2 °K in T_a, 4·1 °K in T_b.

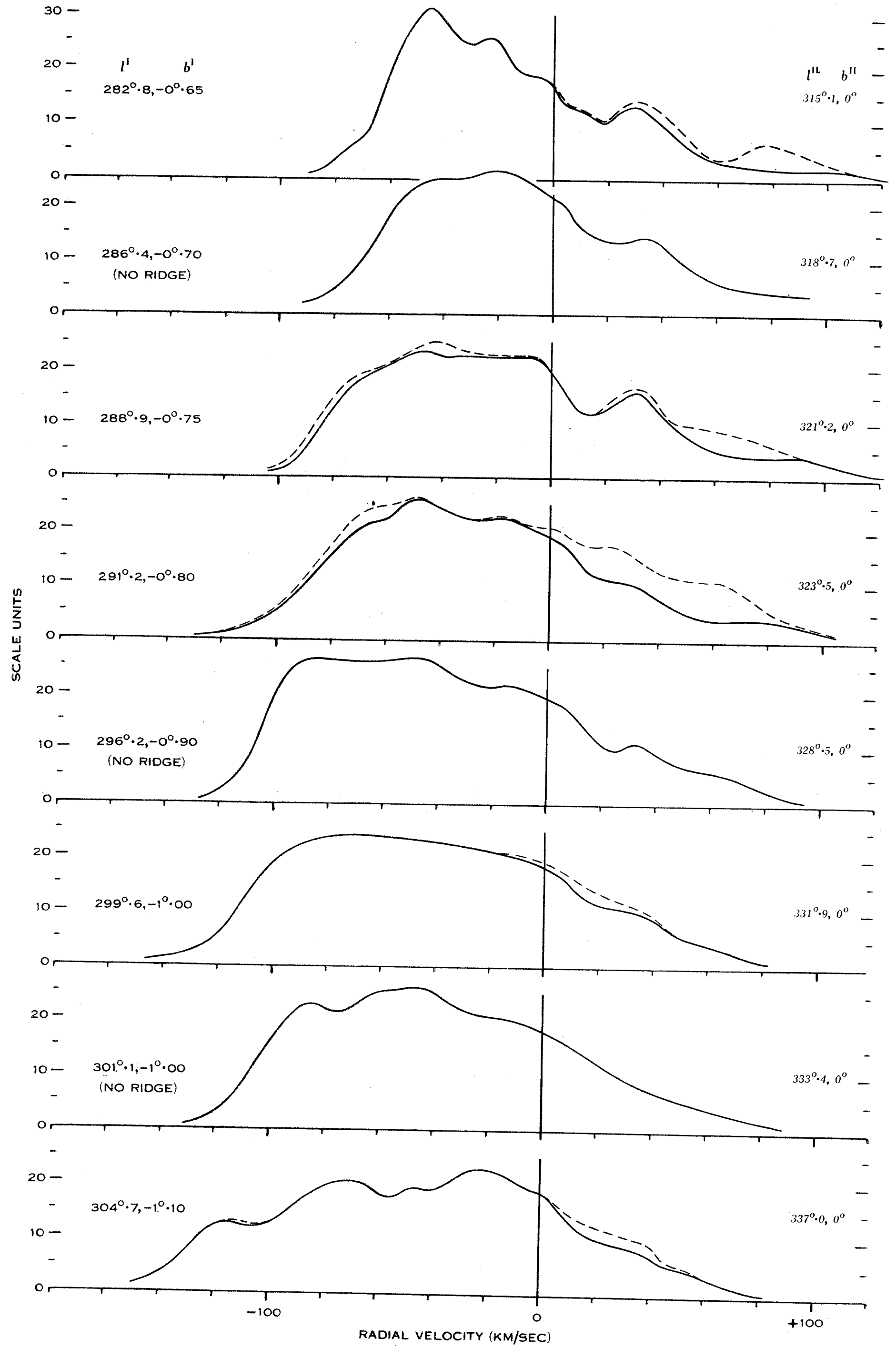

Fig. 10.—Profiles at new galactic equator ———— ; ridge-line profiles (see Section VI (*b*)) – – – – · · · ·. Unit = 3·2 °K in T_a, 4·1 °K in T_b.

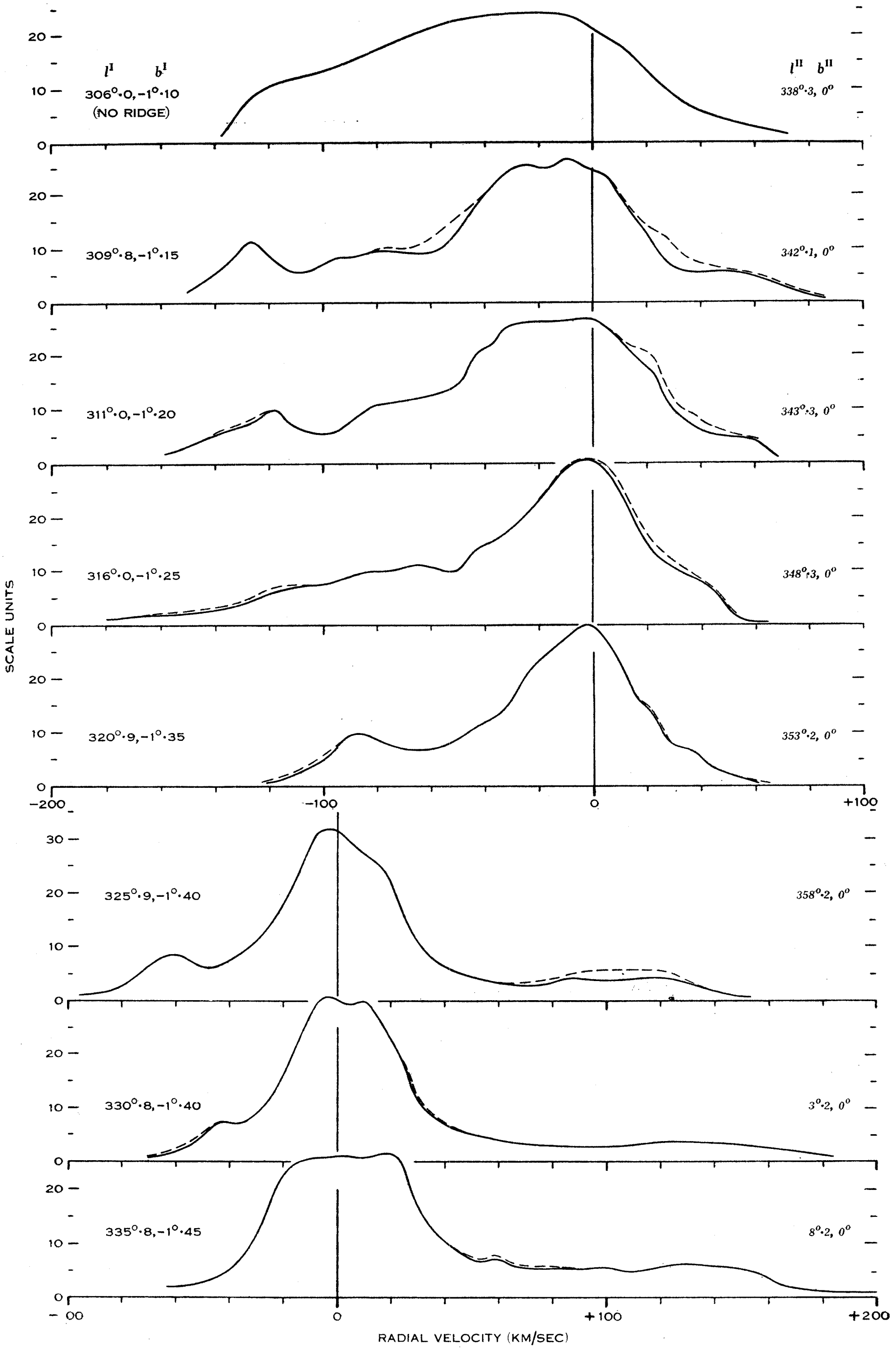

Fig. 11.—Profiles at new galactic equator ———— ; ridge-line profiles (see Section VI (*b*)) – – – · · · ∴ Unit = 3·2 °K in T_a, 4·1 °K in T_b.

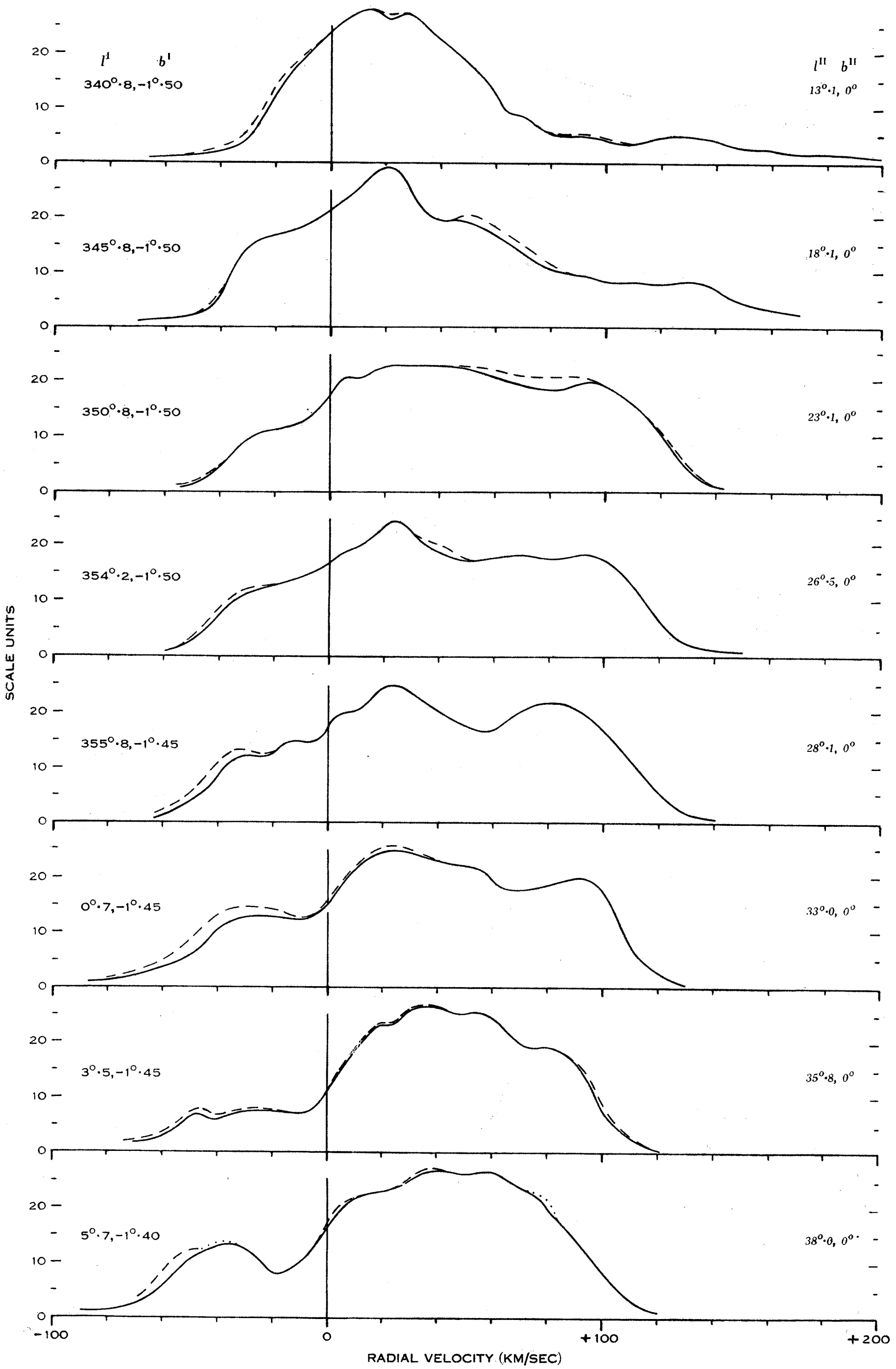

Fig. 12.—Profiles at new galactic equator ———— ; ridge-line profiles (see Section VI (*b*)) – – – · · · ·. Unit = 3·2 °K in T_a, 4·1 °K in T_b.

VI. Results of the Survey

(*a*) *Contour Diagrams*

The full results of the survey are presented in Plates 1–41, in the form of contour diagrams. Each diagram gives the distribution of 21 cm intensity with (old) galactic latitude and radial velocity for a particular track across the Milky Way. The longitude values given are those at which the tracks intersect the old and new galactic equators ; the longitudes at other points on the tracks can be found from Figure 3.

The contour pattern presents the received intensity, with the contour levels marked in scale units ; one unit is equal to 3·2 °K in aerial temperature, and 4·1 °K in brightness temperature. No corrections have been made for aerial smoothing or for continuum radiation. The zero of the intensity scale is the mean of the levels at the two galactic poles at the velocity concerned. The contour lines are dashed in regions where they are least accurate on present evidence.

The ridge-line, the line joining the maxima of the crossing-curves, has been included where possible on each diagram, as this line has special significance in galactic plane considerations. In general, the intensity labels attached to the contours lie on the ridge-line, with the centre of the circle at the point of intersection of the contour line and the ridge-line.

Contour diagrams of this form were selected as the most efficient way of displaying a large amount of information ; line profiles are horizontal cross sections on these diagrams.

(*b*) *A Set of Profiles*

One set of profiles is also given, to aid in quick visualization, especially for demonstrating the change with longitude (see Figs. 8–12). For this purpose, profiles at points along the new galactic equator ($b^{\mathrm{II}}=0$) are the most useful. Both old and new coordinates are given in each case for the point concerned, and also the point is indicated on the latitude scale of the corresponding contour diagram, as a cross reference.

The " ridge-line profile " is also shown for each track ; this curve may be regarded as the upper envelope of the family of profiles for the track concerned, or as the variation of intensity with velocity along the ridge-line of the corresponding contour diagram. It is generally shown as a dashed line, but is in dotted form in places where it is ill defined. In many places the ridge-line profile is almost identical with the galactic equator profile. In such regions the dashed line representing the ridge-line profile is discontinued, but it is to be understood as continuing along the course of the galactic equator profile. The variation of latitude and longitude along the ridge-line has been ignored in the labelling of these profiles, which are identified by the coordinates of the new galactic plane.

VII. Assessment of Results

Gathering together the earlier estimates of measuring accuracy, we have the following values for the estimated probable errors :

Position : $\pm 0^\circ \cdot 07$ in each coordinate.
Velocity : $\pm 0 \cdot 2$ km/sec.

Temperature: ± 2 °K in zero level; ± 7 per cent. in scale factor, for relative measurements; ± 15 per cent. for absolute measurements of aerial temperature; ± 20 per cent. for absolute measurements of brightness temperature.

In addition, the quoted temperatures are subject to inaccuracies which may be introduced in the reduction processes, through the methods used in combining a number of runs. In particular, profiles will be less accurate than sections,

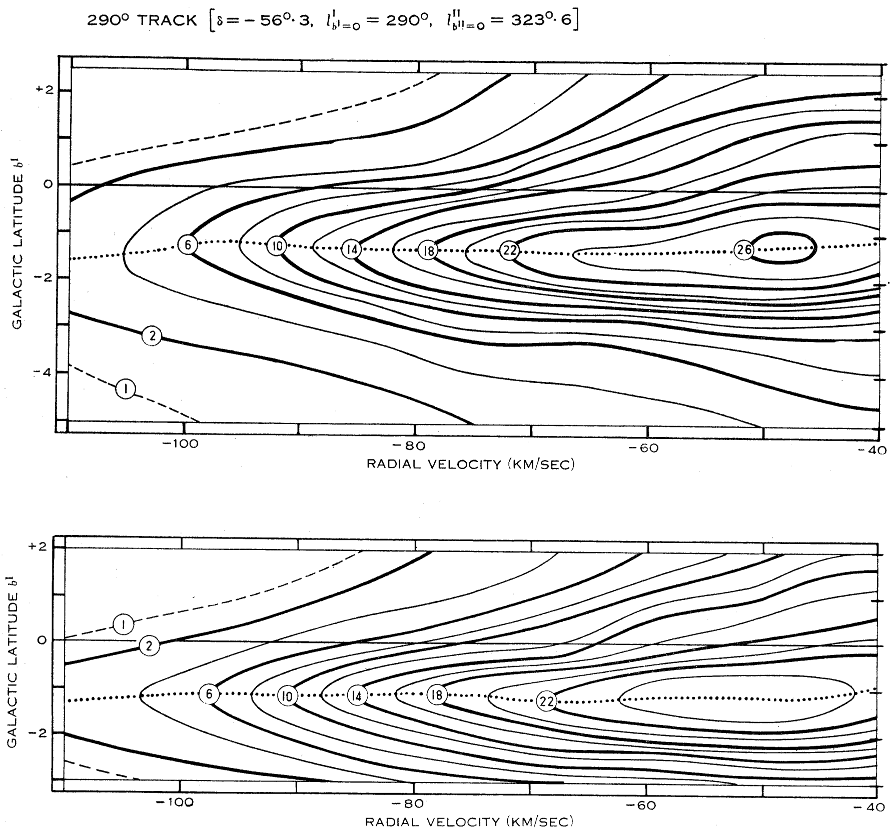

Fig. 13.—Comparison between portions of two independently derived contour diagrams for the 290° track.

because they were built up from a number of observations at discrete frequencies, taken on different days, whereas the sections were recorded directly as continuous curves. The averaging processes will have produced some smoothing in the profiles.

An overall assessment can best be made through comparisons with other sets of results. For this reason, two completely independent sets of observations were taken for the 290° track, and a comparison between them demonstrates the degree of reproducibility of the results. The two contour diagrams are shown in Figure 13, and the two ridge-line profiles in Figure 14.

In addition, the Sydney profiles have been compared with those from the Leiden survey over the whole region of overlap; two examples are shown in Figure 15. The bandwidths were about the same in the two surveys; the beam-widths, however, were significantly different, 1°·4 by 1°·4 for Sydney, and 1°·8 by 2°·8 for Leiden (Kootwijk).

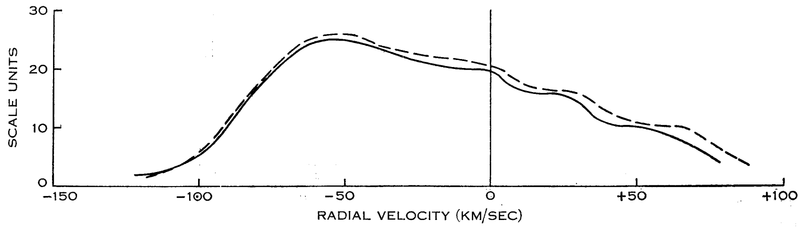

Fig. 14.—Two ridge-line profiles for the same track, derived from independent sets of observations (290° track).

The velocity scales are found to agree quite closely. In a comparison of the intensity scales, an average taken over the central parts of the profiles for the whole overlap region gave a value of 1·28 for the ratio of Sydney brightness temperatures to Leiden published temperatures. There are large uncertainties in both temperature scales, but the absolute values of the temperatures are less important than the need to establish a consistent temperature scale for combining the Sydney and Leiden surveys.

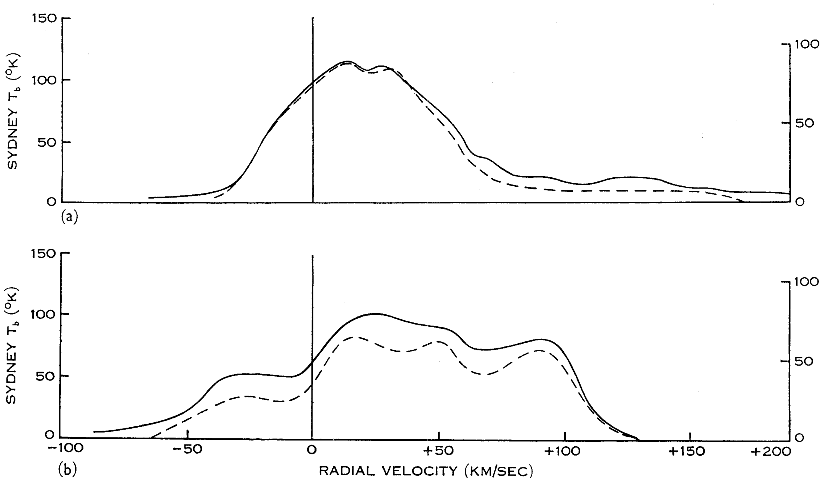

Fig. 15.—Sample comparisons between Sydney and Leiden profiles. ——— Sydney; – – – – Leiden. (*a*) $l^{\mathrm{I}}=340°\cdot 9$, $b^{\mathrm{I}}=-1°\cdot 6$; (*b*) $l^{\mathrm{I}}=0°\cdot 9$, $b^{\mathrm{I}}=-1°\cdot 6$.

There is reasonable agreement between the shapes of the Sydney and Leiden profiles, but the Sydney ones may have some additional smoothing, resulting from the method of derivation. On the other hand, the variation with latitude should be more reliable in the Sydney case. There is a tendency for the Sydney intensities to be relatively higher in the wings of the profiles; this appears to be mainly due to the higher resolution in latitude, since the angle subtended by the gas layer is smallest for the higher velocities.

The two sets of results are sufficiently homogeneous to be used together for building up an overall picture of the whole Galaxy. Although it would be desirable to have a closer sampling in longitude and a wider coverage in latitude, the information which is now available is adequate for deriving a coarse picture of galactic structure. This subject, and other aspects of the analysis, will be taken up in subsequent papers.

VIII. Acknowledgments

B. J. Robinson, Mrs. Martha Stahr Carpenter, and R. L. Dowden were associated with the project in various periods and made substantial contributions. E. C. Holmes carried out a large part of the later observations and equipment maintenance; Miss Pat Healy did a major share of the computational work; and Miss Elaine Mapledorum and Mrs. Susan Paterson traced the diagrams.

IX. References

Blaauw, A., Gum, C. S., Pawsey, J. L., and Westerhout, G. (1959).—*I.A.U. Inform. Bull.* No. 1: 4–6.

Christiansen, W. N., and Hindman, J. V. (1952).—*Aust. J. Sci. Res.* A **5**: 437–55.

Ewen, H. I., and Purcell, E. M. (1951).—*Nature* **168**: 356.

Gill, M. C. (1955).—C.S.I.R.O. Aust. Div. Radiophys. Rep. RPL 101.

Gum, C. S., and Kerr, F. J. (1958).—C.S.I.R.O. Aust. Div. Radiophys. Rep. RPL 138.

Gum, C. S., and Pawsey, J. L. (1958).—C.S.I.R.O. Aust. Div. Radiophys. Rep. RPL 137.

Hindman, J. V., and Wade, C. M. (1959).—*Aust. J. Phys.* **12**: 258–69.

van de Hulst, H. C., Muller, C. A., and Oort, J. H. (1954).—*Bull. Astr. Insts. Netherlds.* **12**: 117–49.

Kerr, F. J., Hindman, J. V., and Carpenter, M. S. (1957).—*Nature* **180**: 677–9.

Kerr, F. J., Hindman, J. V., and Robinson, B. J. (1954).—*Aust. J. Phys.* **7**: 297–314.

Muller, C. A., and Westerhout, G. (1957).—*Bull. Astr. Insts. Netherlds.* **13**: 151–95.

Ohlsson, J. (1932).—*Ann. Lund Obs.* No. 3.

Oort, J. H., Kerr, F. J., and Westerhout, G. (1958).—*Mon. Not. R. Astr. Soc.* **118**: 379–89.

Schmidt, M. (1957).—*Bull. Astr. Insts. Netherlds.* **13**: 247–68.

Seeger, C. L., Westerhout, G., and van de Hulst, H. C. (1956).—*Bull. Astr. Insts. Netherlds.* **13**: 89–99.

Westerhout, G. (1957).—*Bull. Astr. Insts. Netherlds.* **13**: 201–46.

Explanation of Plates 1–41

Contour diagrams showing distribution of 21 cm radiation along 41 tracks crossing the Southern Milky Way.

Contours are of constant 21 cm intensity;

1 unit $=3\cdot2$ °K in aerial temperature

$=4\cdot1$ °K in brightness temperature.

Tracks.—All but six of the tracks are along constant declination lines.

The 175° track is at $\delta=+4°\cdot4$ (1955); it crosses the old galactic equator at $l^{\mathrm{I}}=175°$ and the new equator at $l^{\mathrm{II}}=208°\cdot1$.

The tracks are not normal to the galactic equator, but in most cases cross it at steep angles. Details of all tracks are given in Figure 3 and the declination formulae for the tracks in Plates 13–18 are in Table 2.

For full description see Section VI (*a*).

21 CM SURVEY OF THE SOUTHERN MILKY WAY

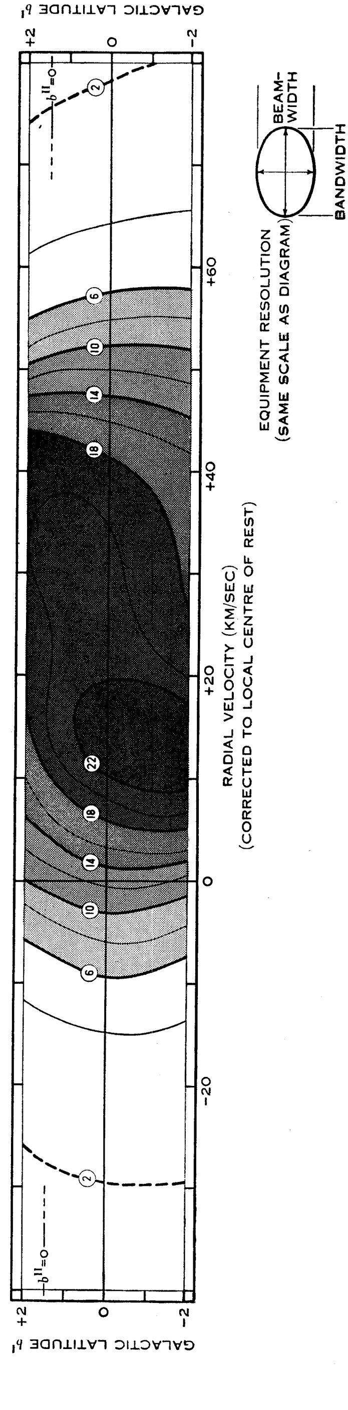

175° TRACK $\left[\delta = +4°.4,\ l^{I}_{b^{I}=0} = 175°,\ l^{II}_{b^{II}=0} = 208°.1\right]$

21 CM SURVEY OF THE SOUTHERN MILKY WAY

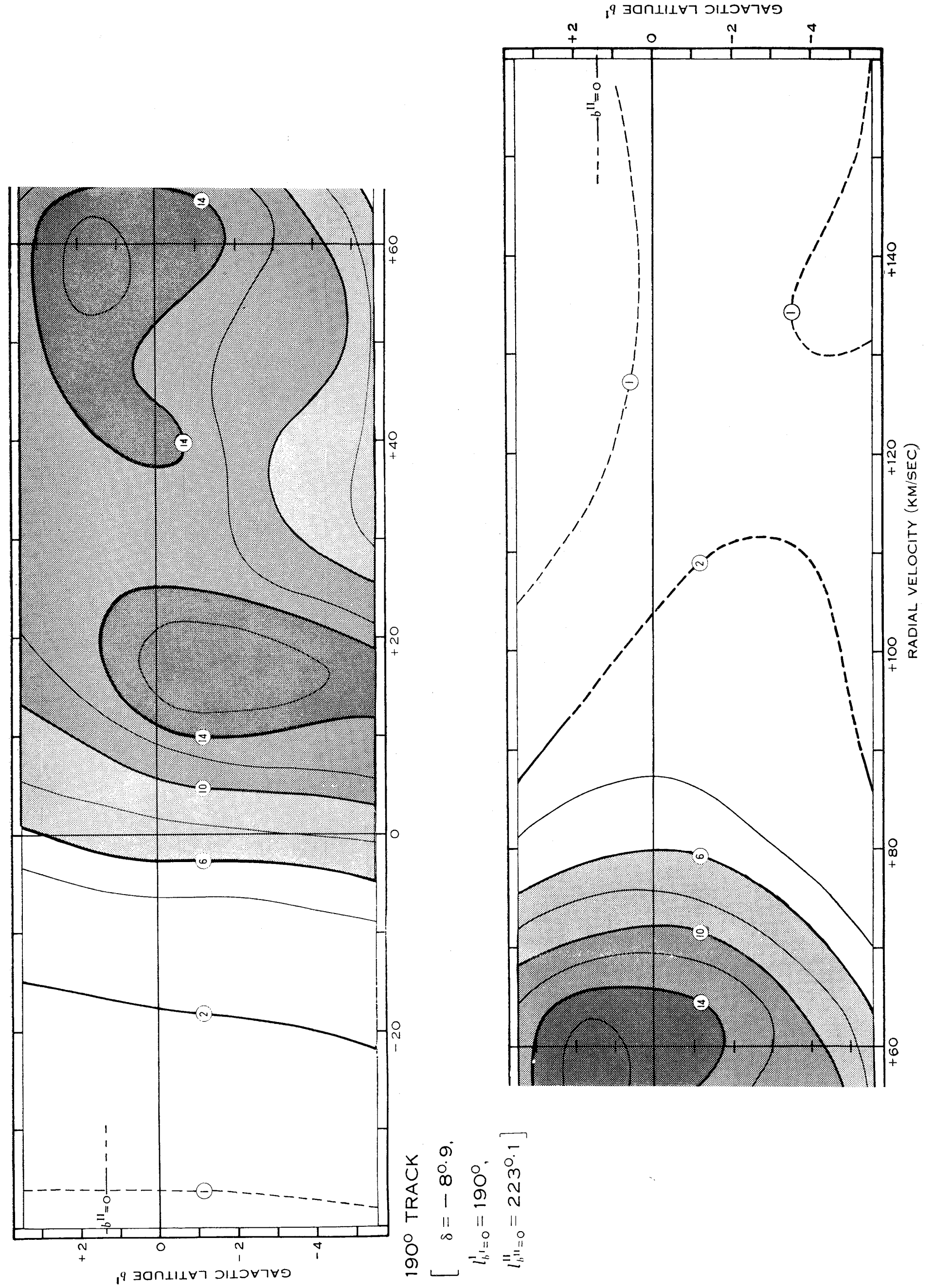

190° TRACK
[$\delta = -8^{\circ}.9$, $l^{I}_{b^{I}=0} = 190^{\circ}$, $l^{II}_{b^{II}=0} = 223^{\circ}.1$]

21 CM SURVEY OF THE SOUTHERN MILKY WAY

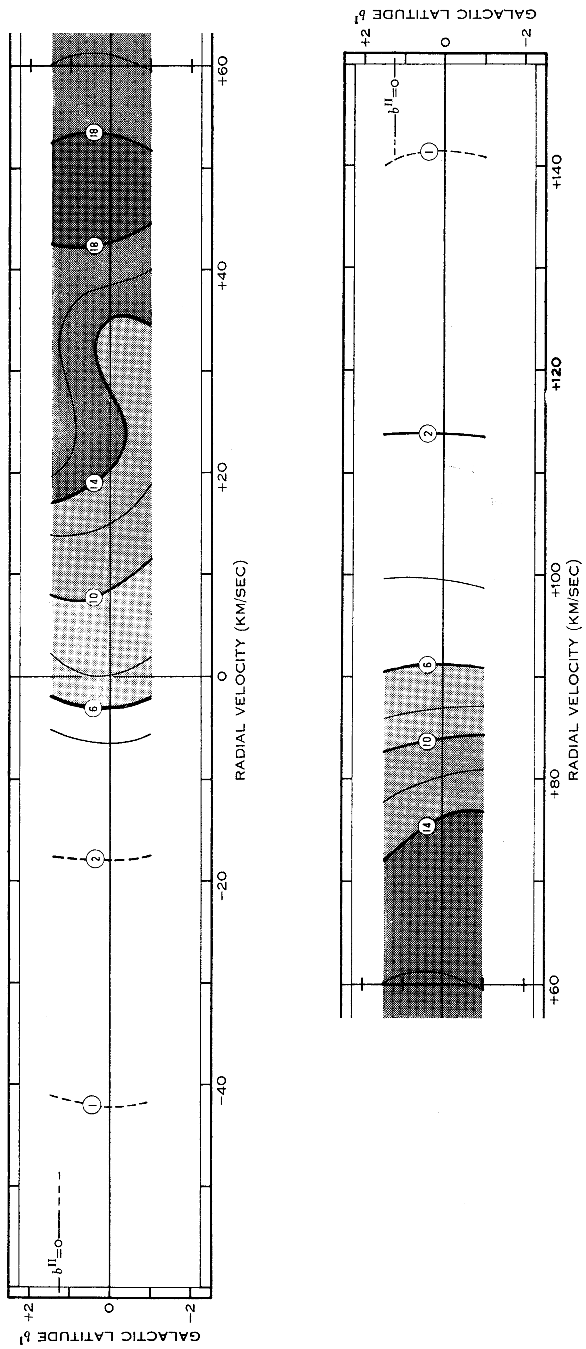

200° TRACK [$\delta = -17°.7$, $l^{I}_{b^{I}=0} = 200°$, $l^{II}_{b^{II}=0} = 233°.0$]

21 CM SURVEY OF THE SOUTHERN MILKY WAY

210° TRACK $\left[\delta = -26°.3,\ l^{I}_{b^{I}=0} = 210°,\ l^{II}_{b^{II}=0} = 243°.0\right]$

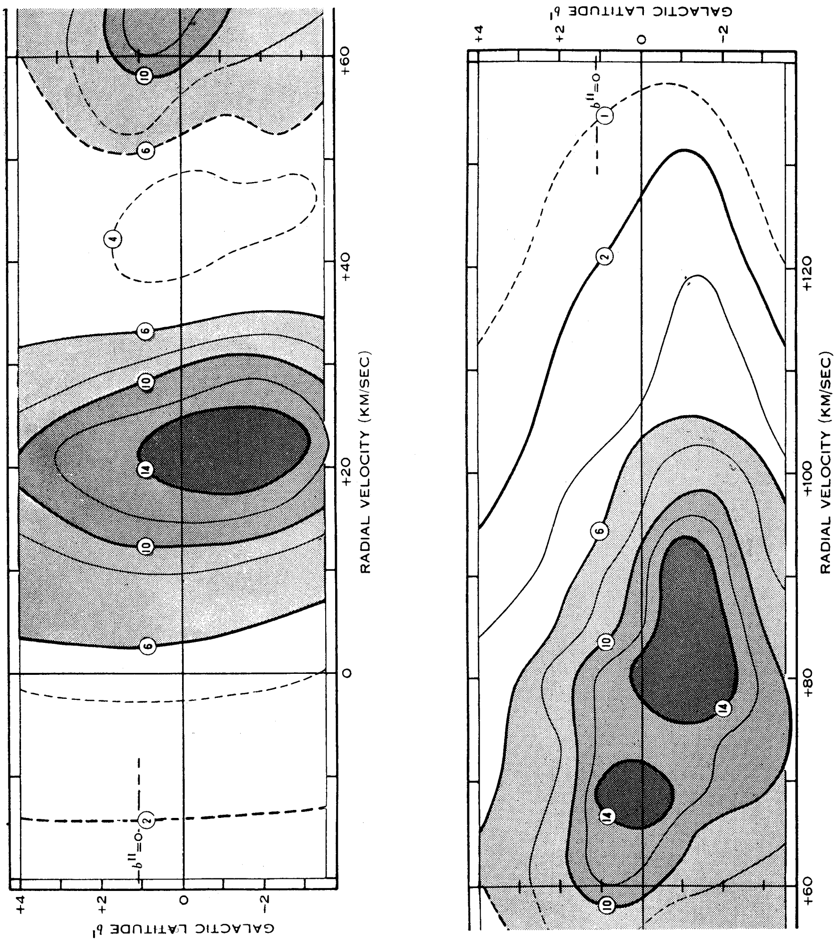

21 CM SURVEY OF THE SOUTHERN MILKY WAY

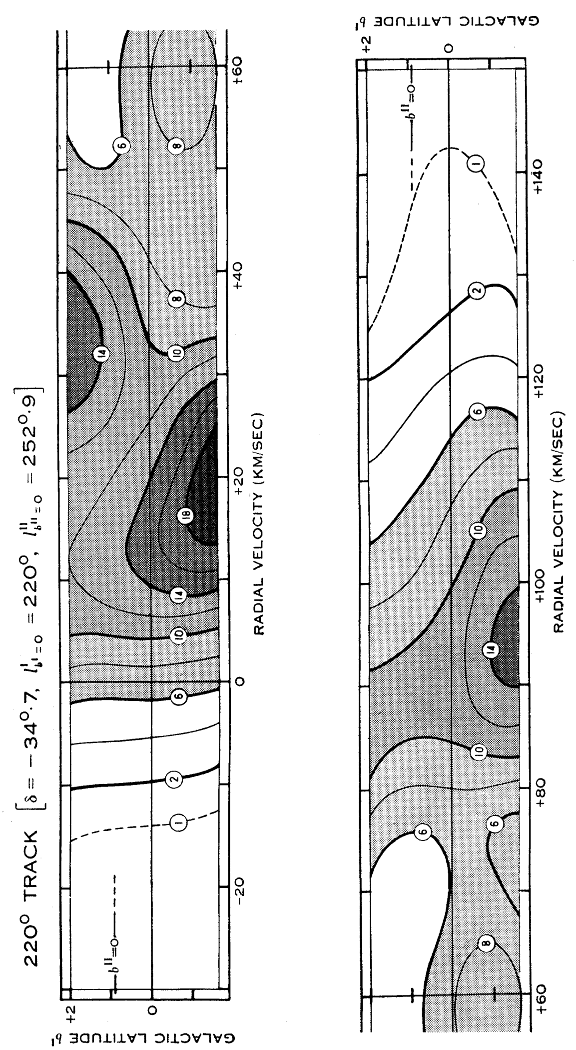

21 CM SURVEY OF THE SOUTHERN MILKY WAY

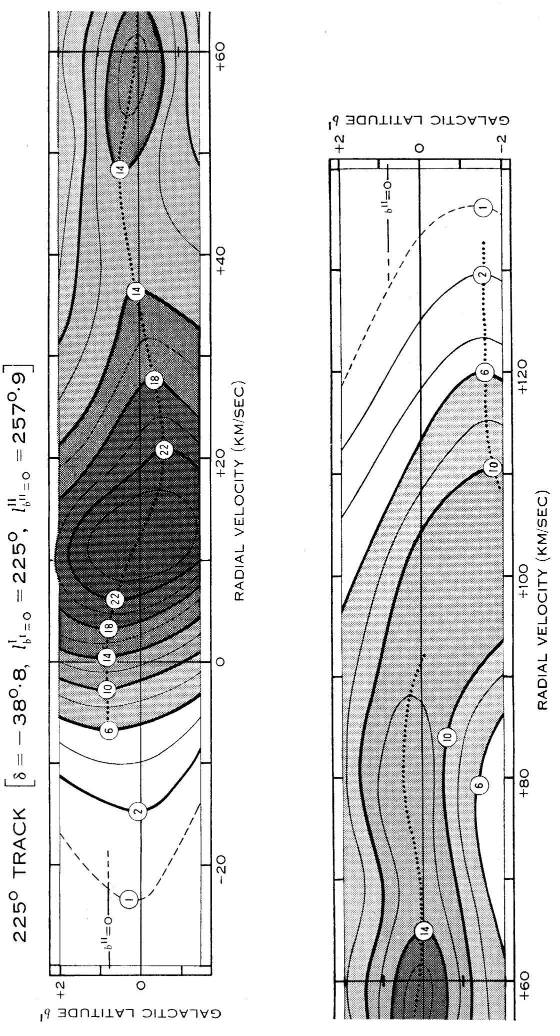

21 CM SURVEY OF THE SOUTHERN MILKY WAY

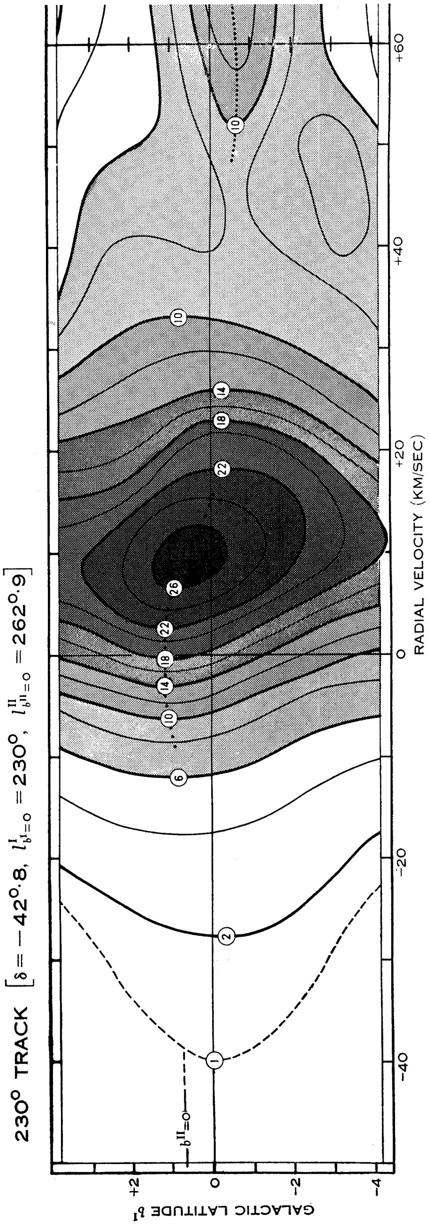

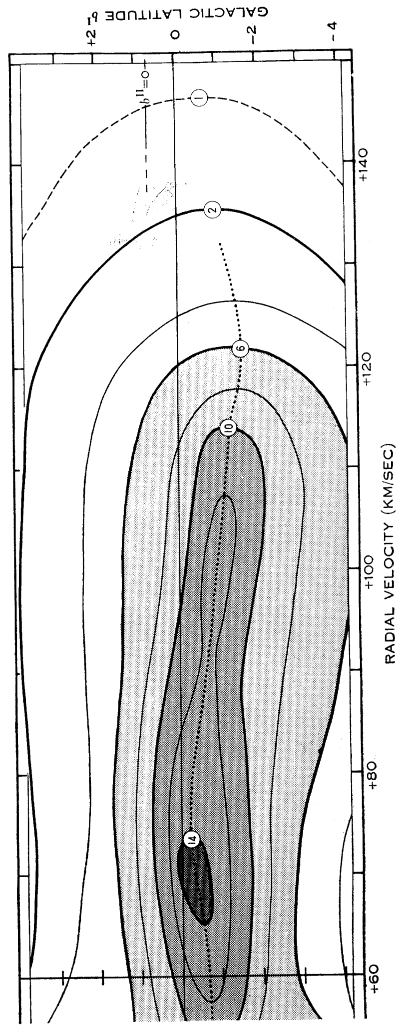

21 CM SURVEY OF THE SOUTHERN MILKY WAY

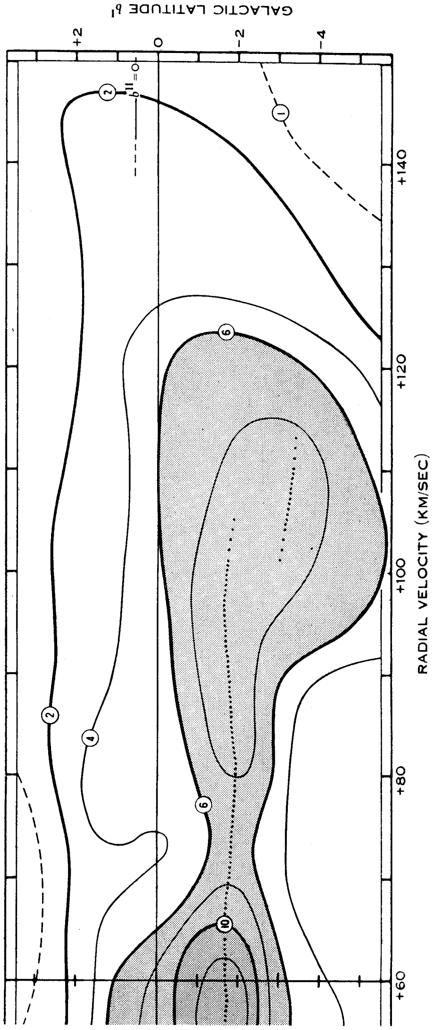

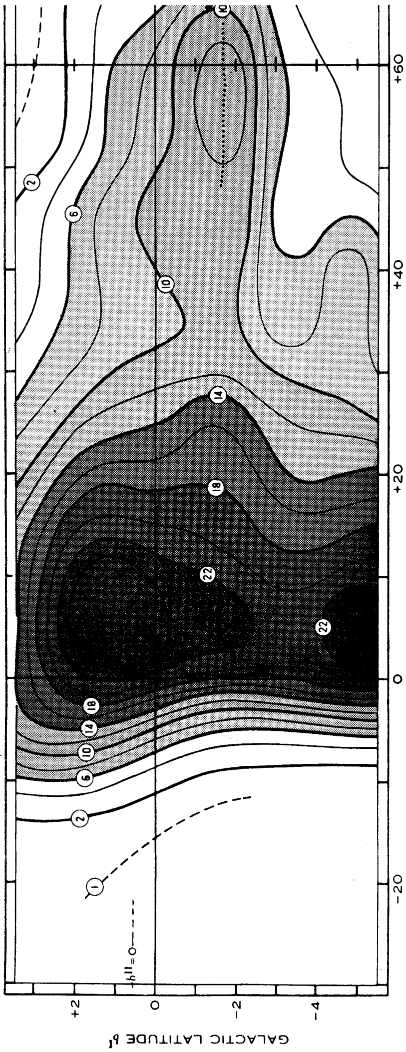

235° TRACK

$\delta = -46°.5$,

$l^I_{b^I=0} = 235°$,

$l^{II}_{b^{II}=0} = 267°.8$

21 CM SURVEY OF THE SOUTHERN MILKY WAY

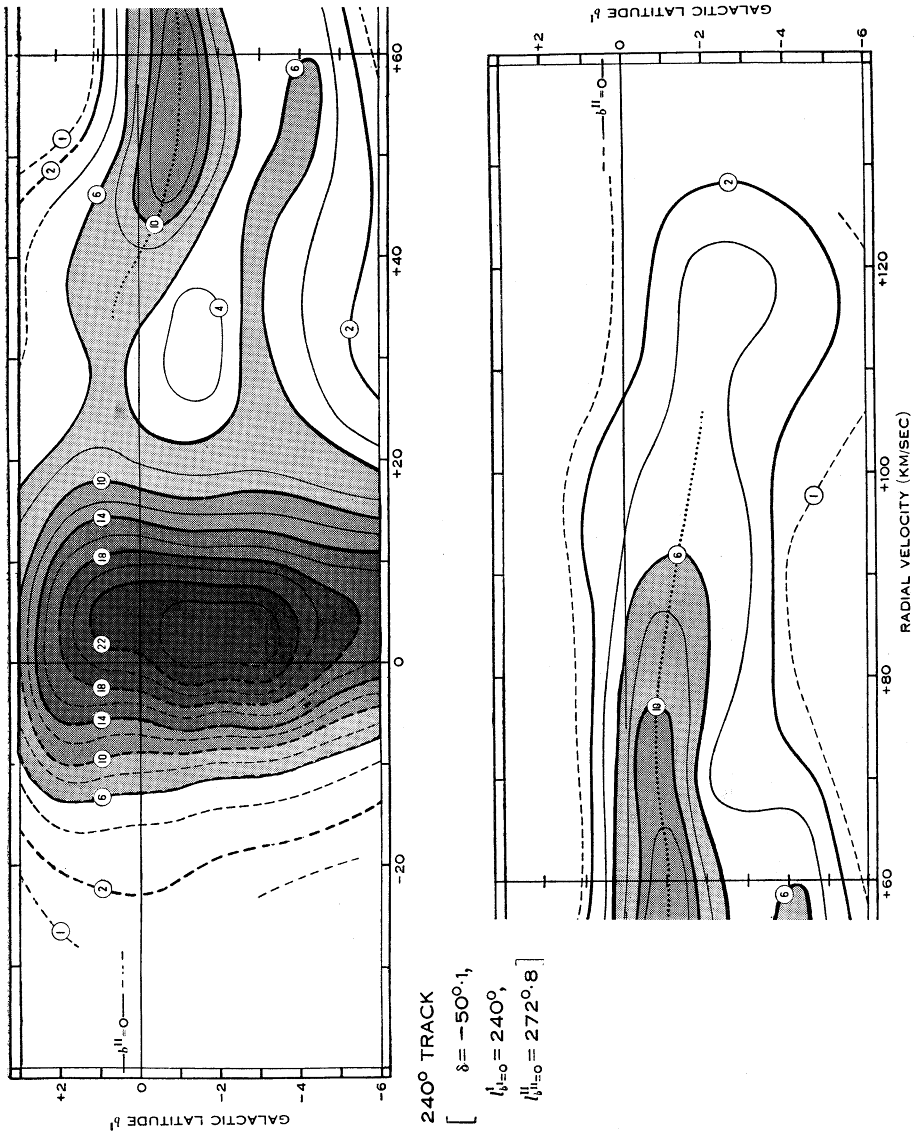

21 CM SURVEY OF THE SOUTHERN MILKY WAY

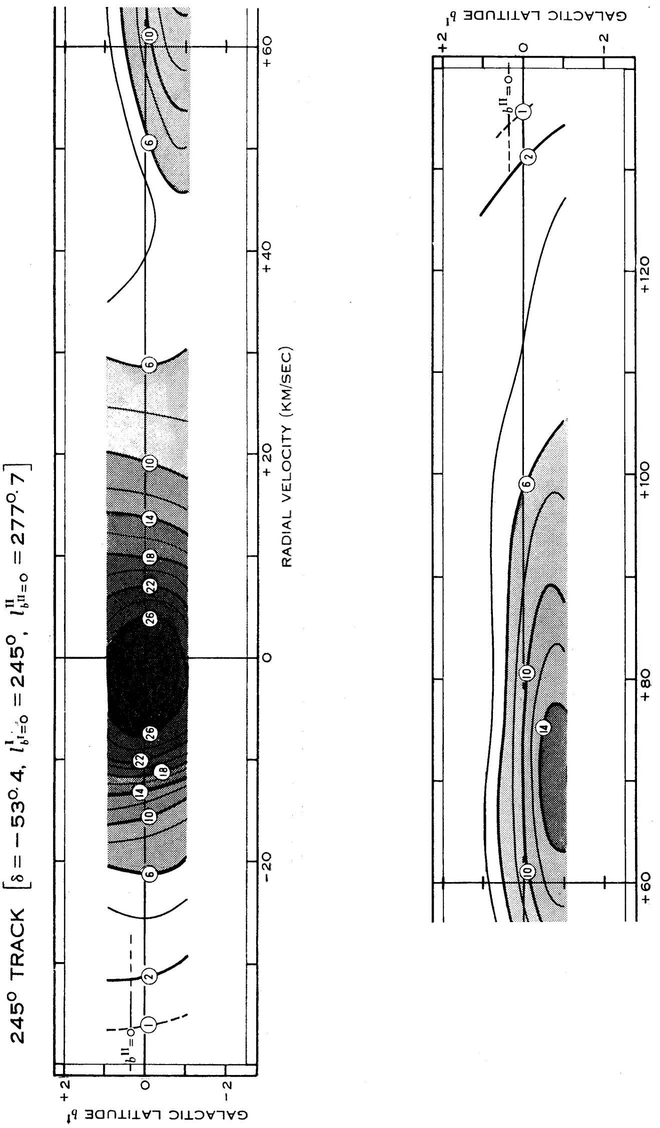

21 CM SURVEY OF THE SOUTHERN MILKY WAY

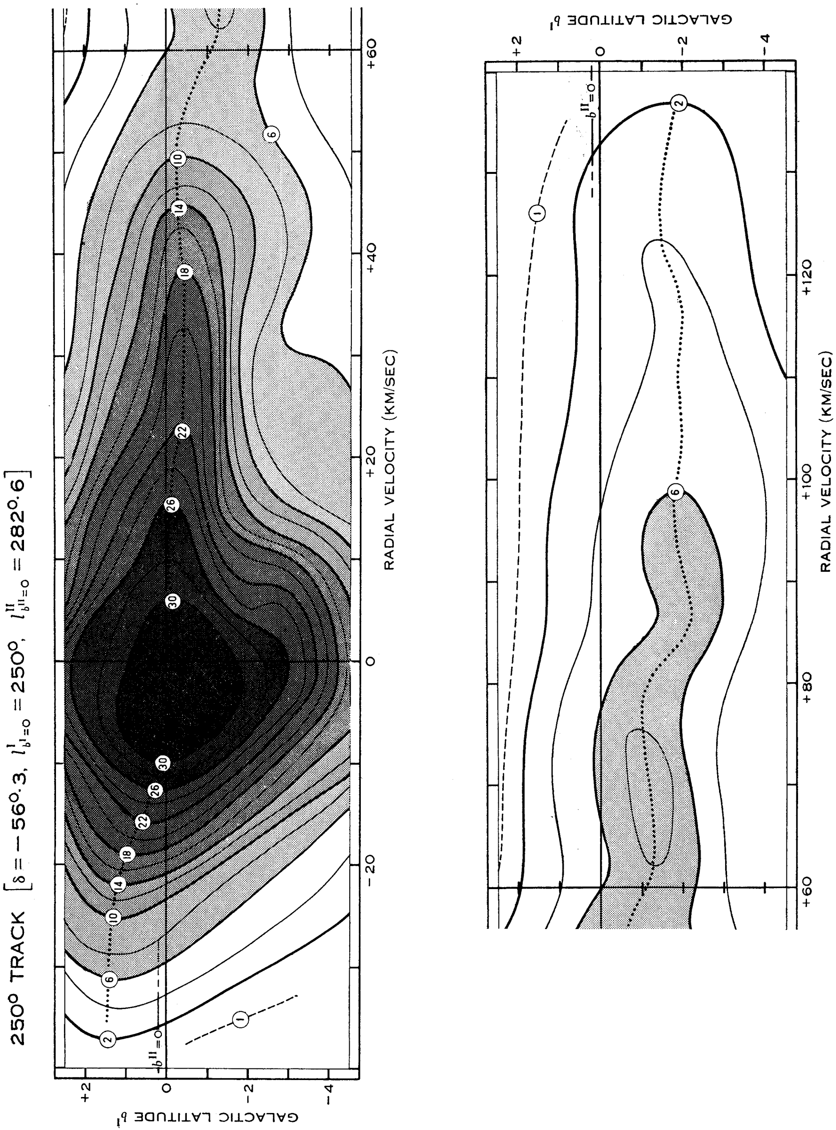

21 CM SURVEY OF THE SOUTHERN MILKY WAY

255° TRACK $\left[\delta = -58°\!\cdot\!8,\ l^{\mathrm{I}}_{b^{\mathrm{I}}=0} = 255°,\ l^{\mathrm{II}}_{b^{\mathrm{II}}=0} = 287°\!\cdot\!4\right]$

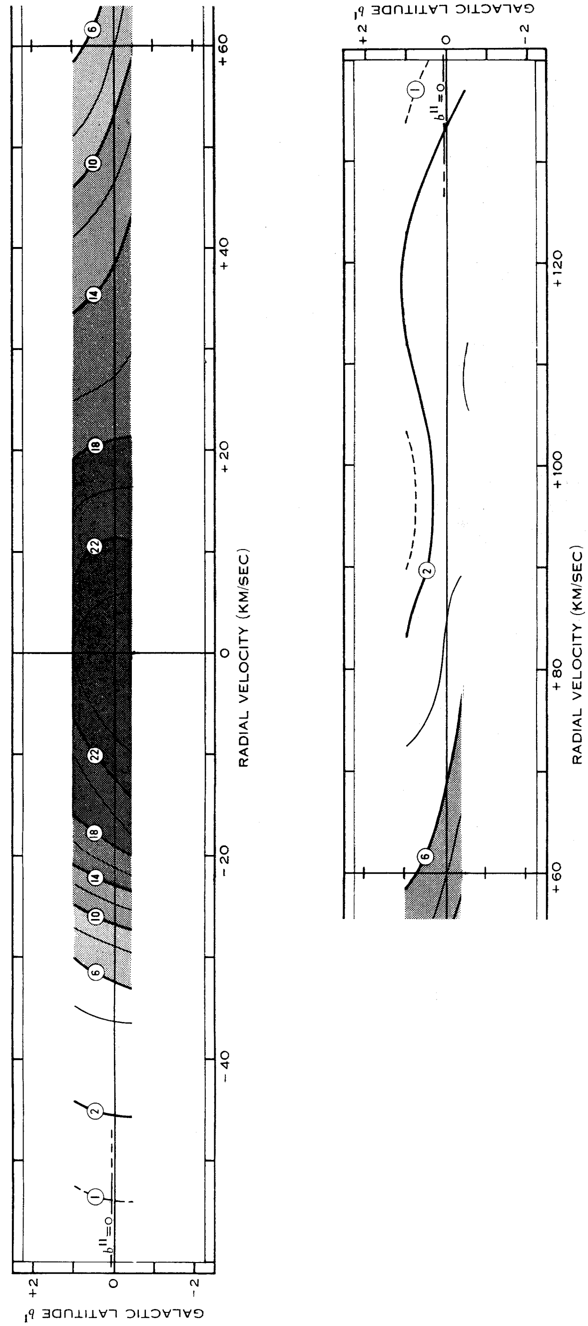

21 CM SURVEY OF THE SOUTHERN MILKY WAY

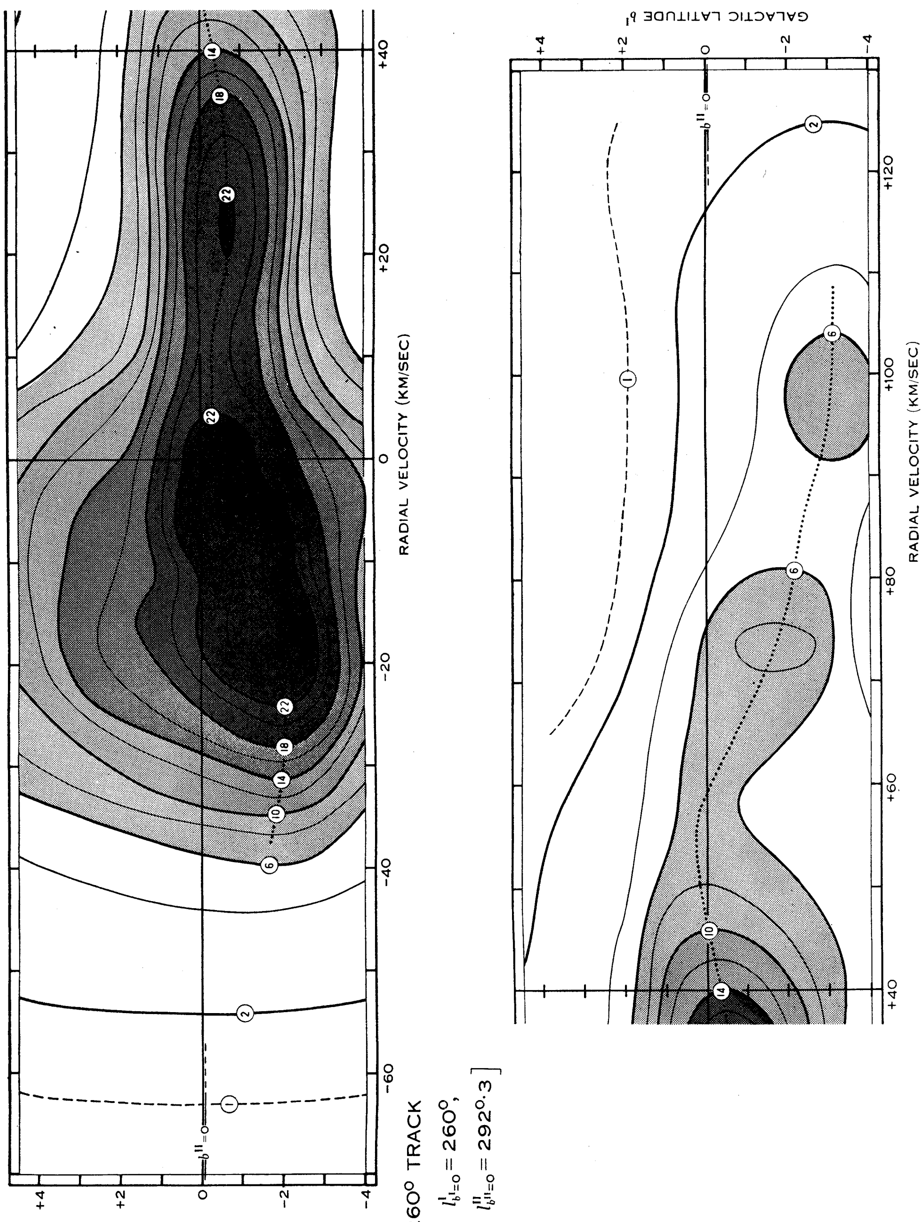

21 CM SURVEY OF THE SOUTHERN MILKY WAY

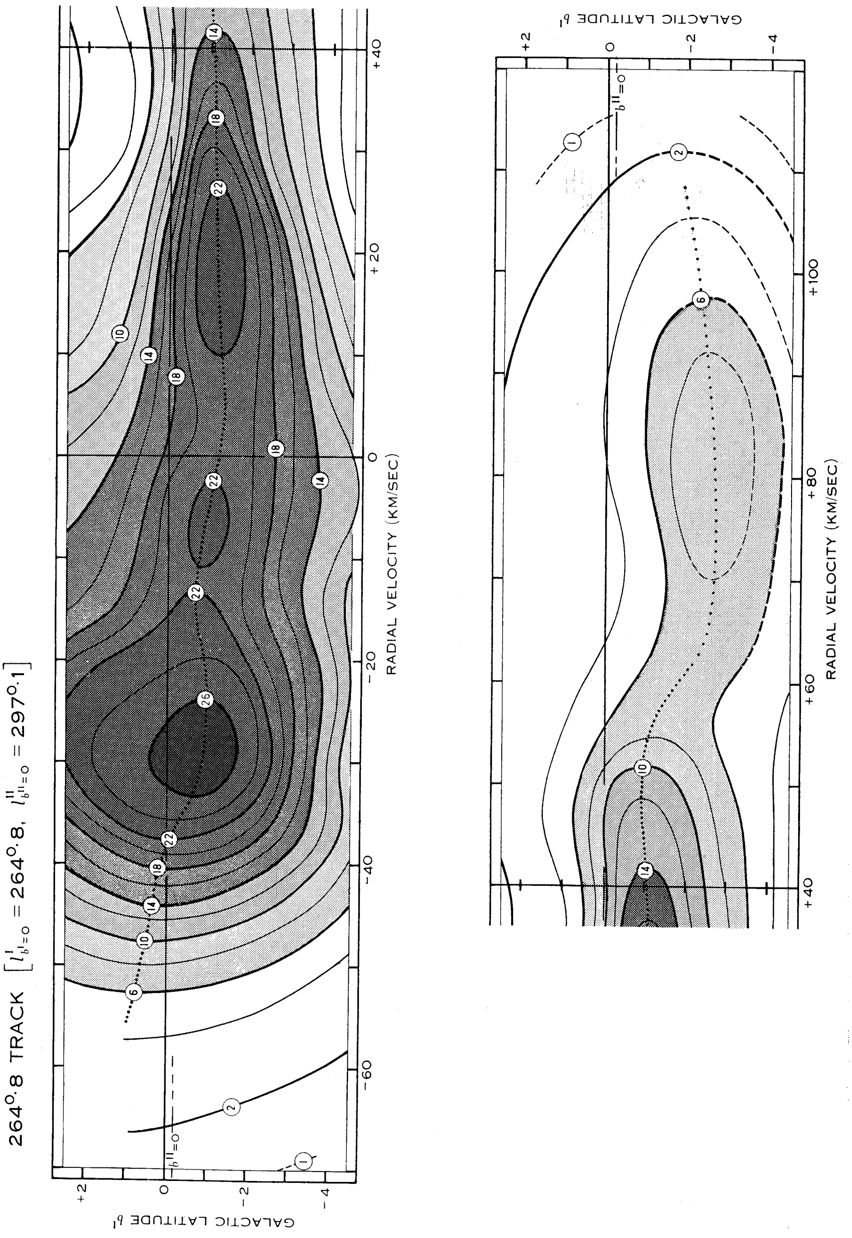

21 CM SURVEY OF THE SOUTHERN MILKY WAY

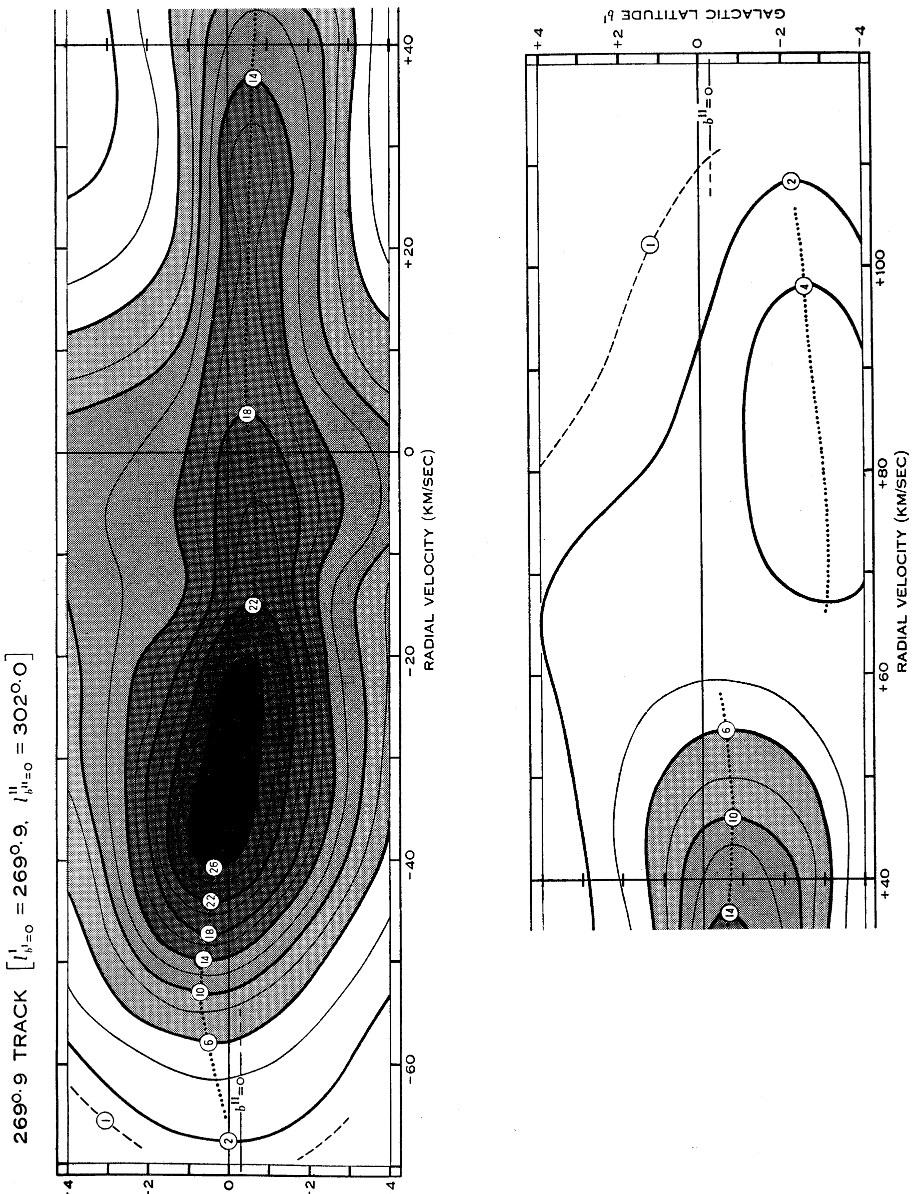

21 CM SURVEY OF THE SOUTHERN MILKY WAY

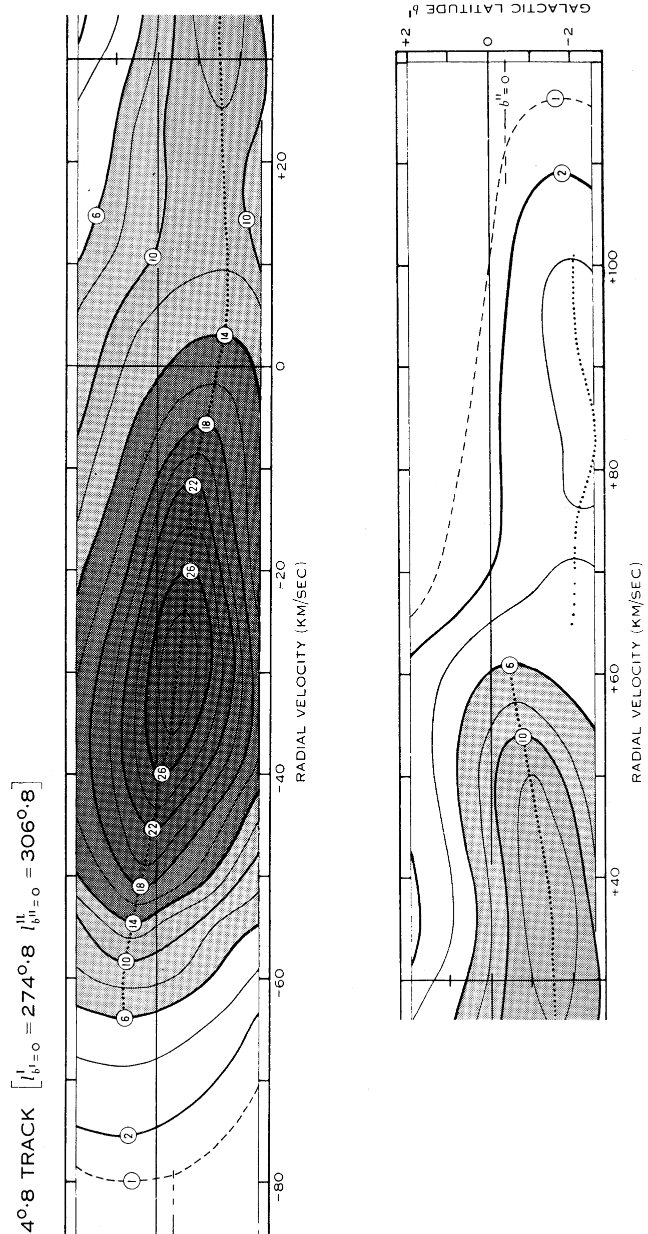

21 CM SURVEY OF THE SOUTHERN MILKY WAY

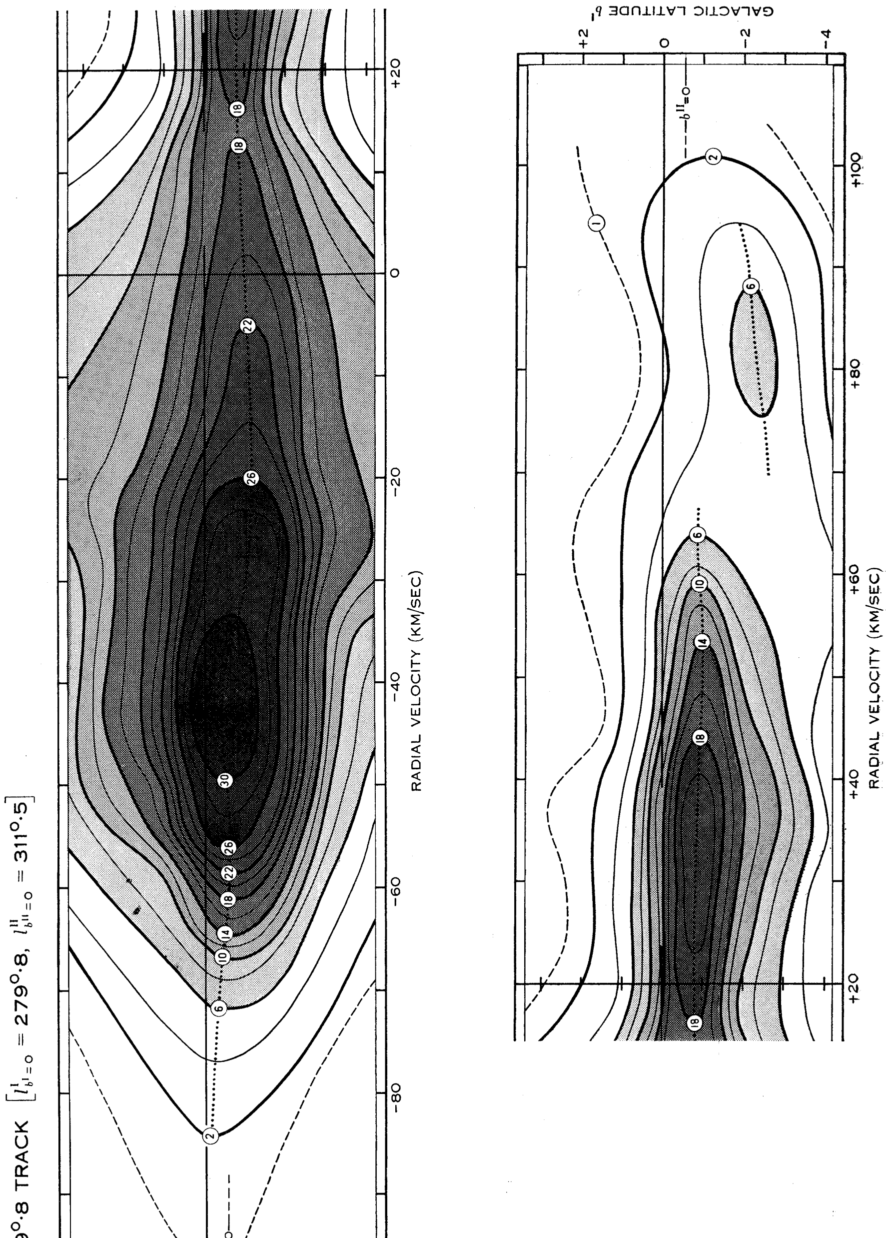

21 CM SURVEY OF THE SOUTHERN MILKY WAY

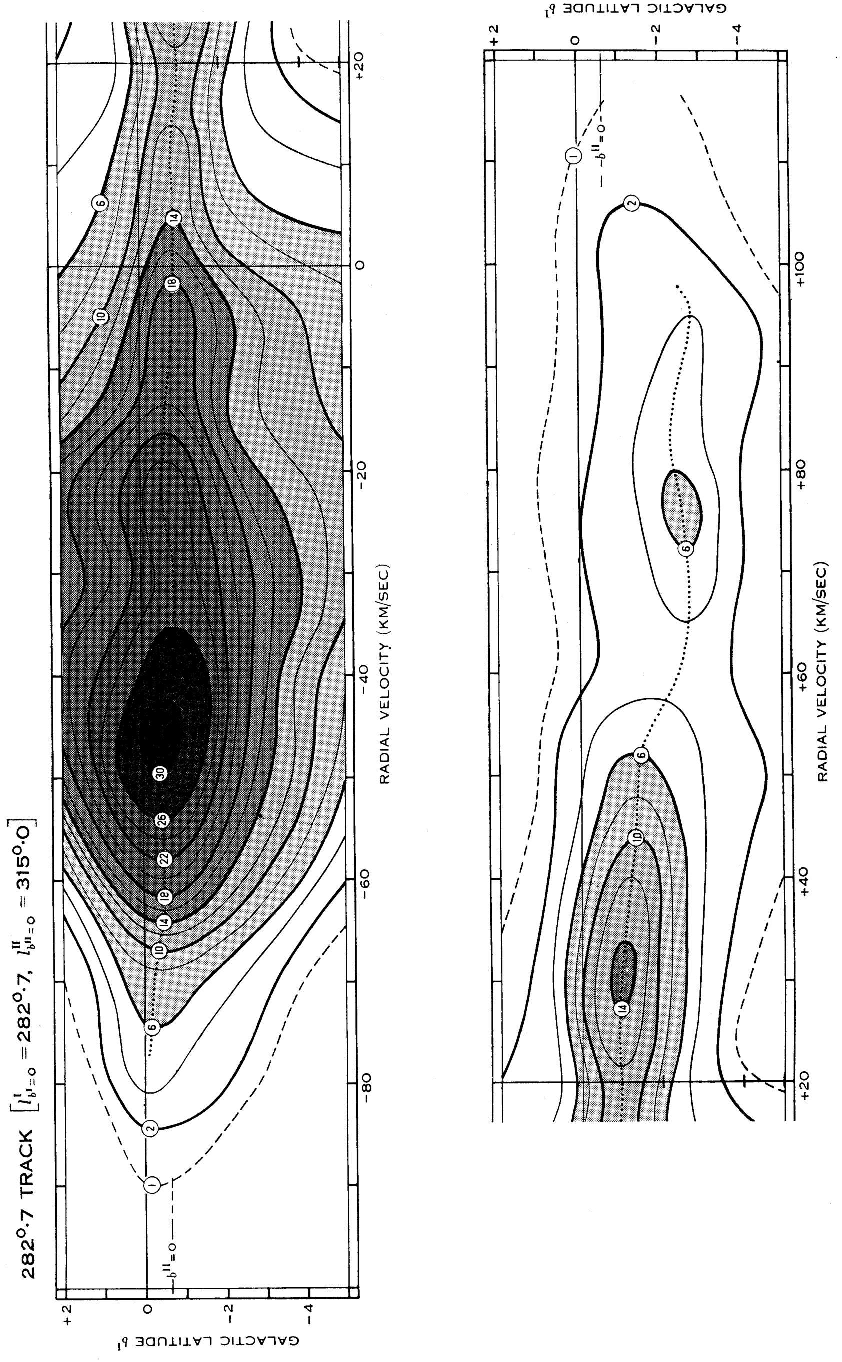

21 CM SURVEY OF THE SOUTHERN MILKY WAY

285° TRACK $\left[\delta = -58^{\circ}\cdot 8,\ l^{\mathrm{I}}_{b^{\mathrm{I}}=0} = 285^{\circ},\ l^{\mathrm{II}}_{b^{\mathrm{II}}=0} = 318^{\circ}\cdot 7\right]$

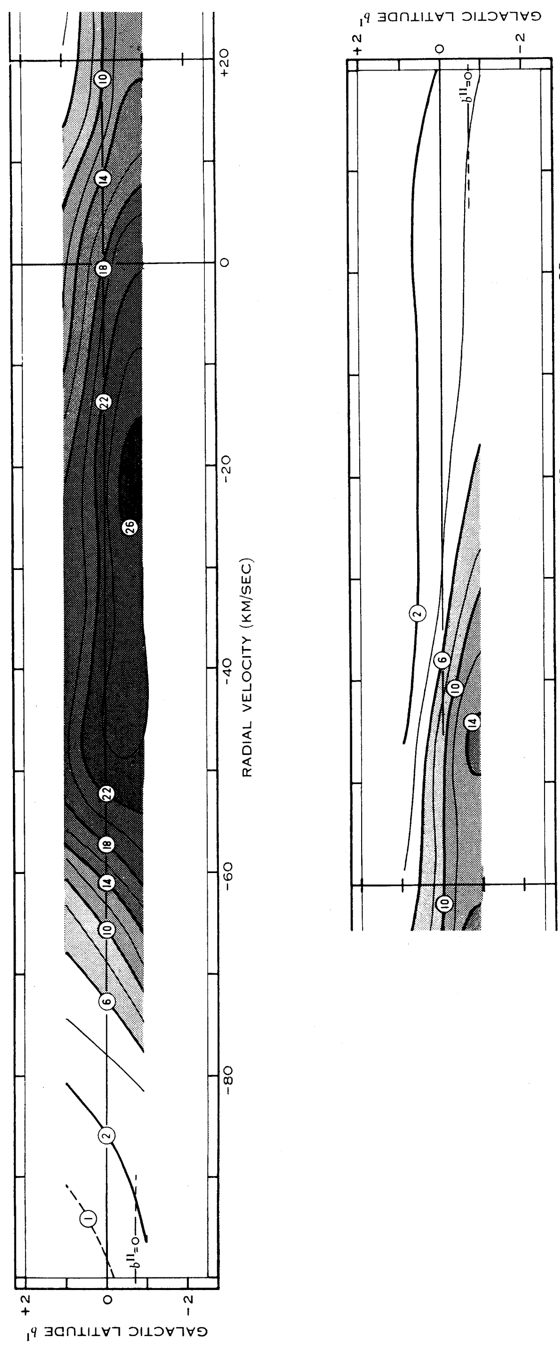

21 CM SURVEY OF THE SOUTHERN MILKY WAY

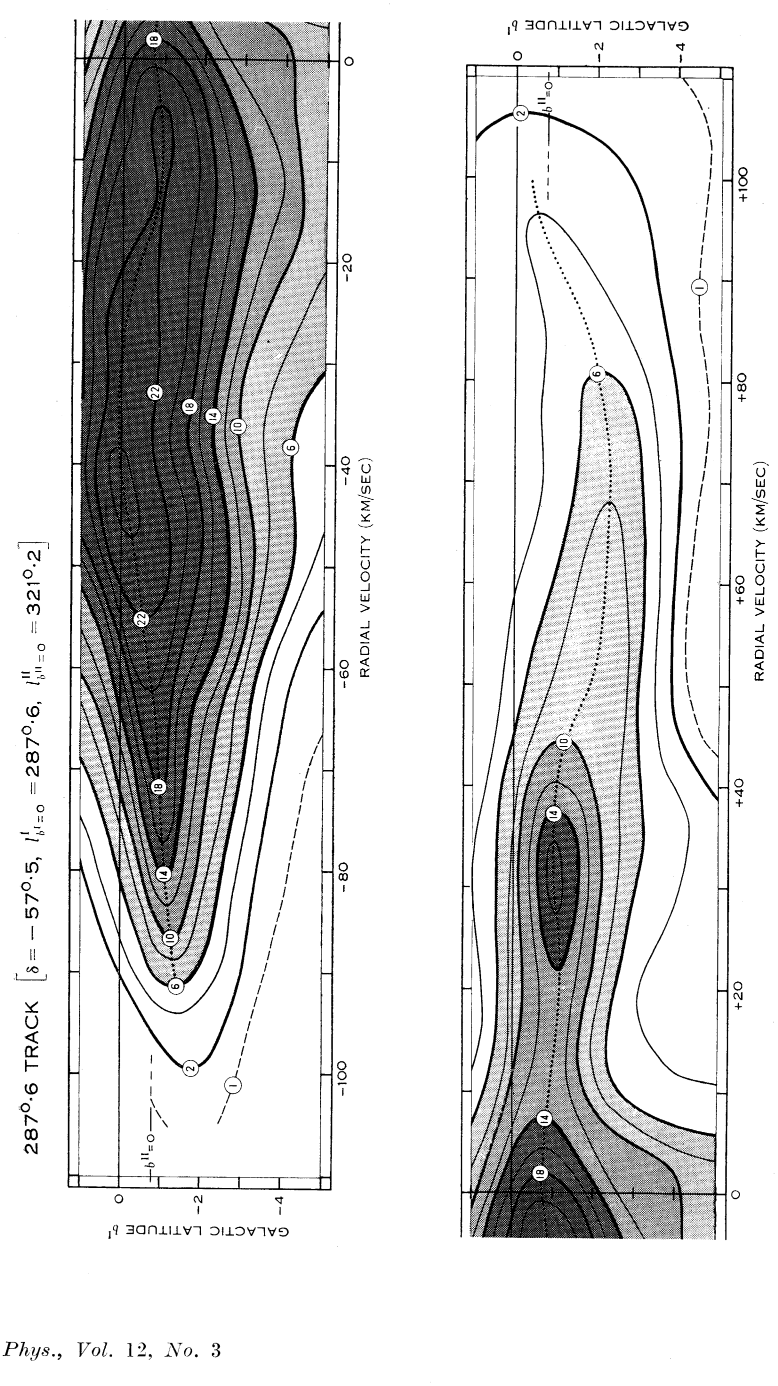

21 CM SURVEY OF THE SOUTHERN MILKY WAY

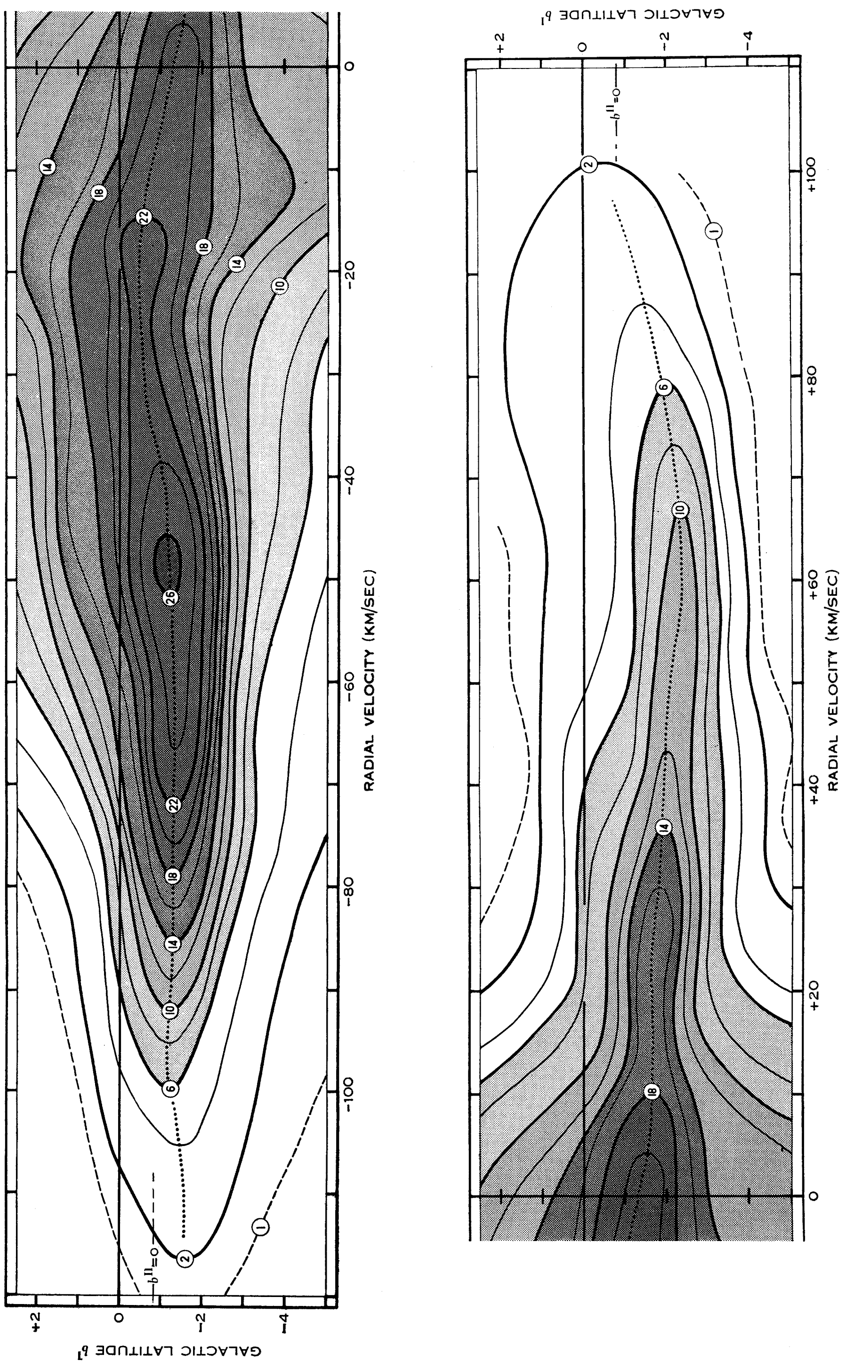

290° TRACK $\left[\delta = -56°.3,\ l^{I}_{b^{I}=0} = 290°,\ l^{II}_{b^{II}=0} = 323°.5\right]$

21 CM SURVEY OF THE SOUTHERN MILKY WAY

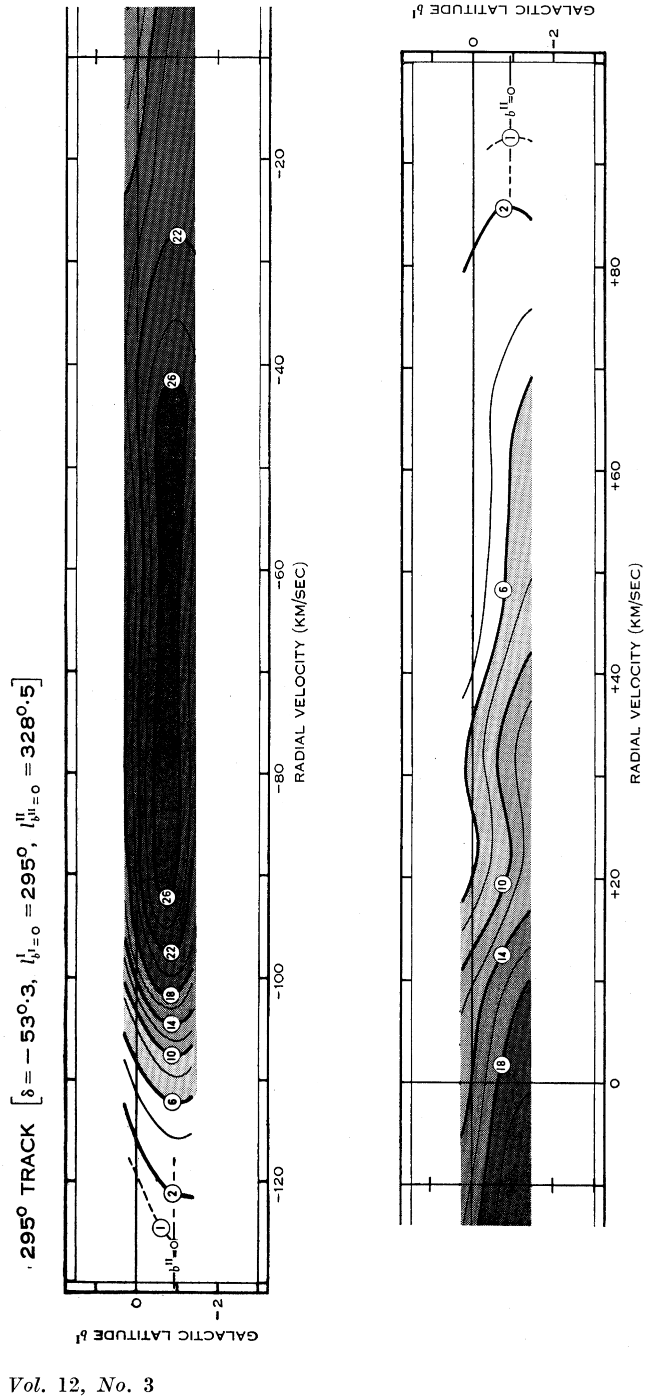

21 CM SURVEY OF THE SOUTHERN MILKY WAY

298°.5 TRACK $[\delta = -51°.0,\ l^{I}_{b^{I}=0} = 298°.5,\ l^{II}_{b^{II}=0} = 331°.9]$

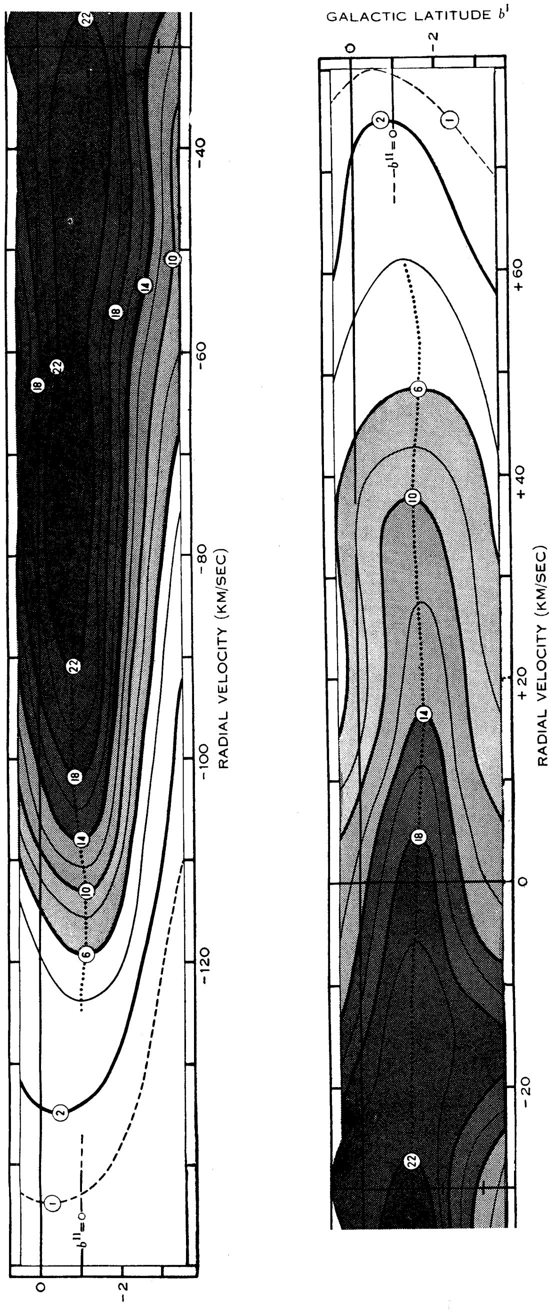

21 CM SURVEY OF THE SOUTHERN MILKY WAY

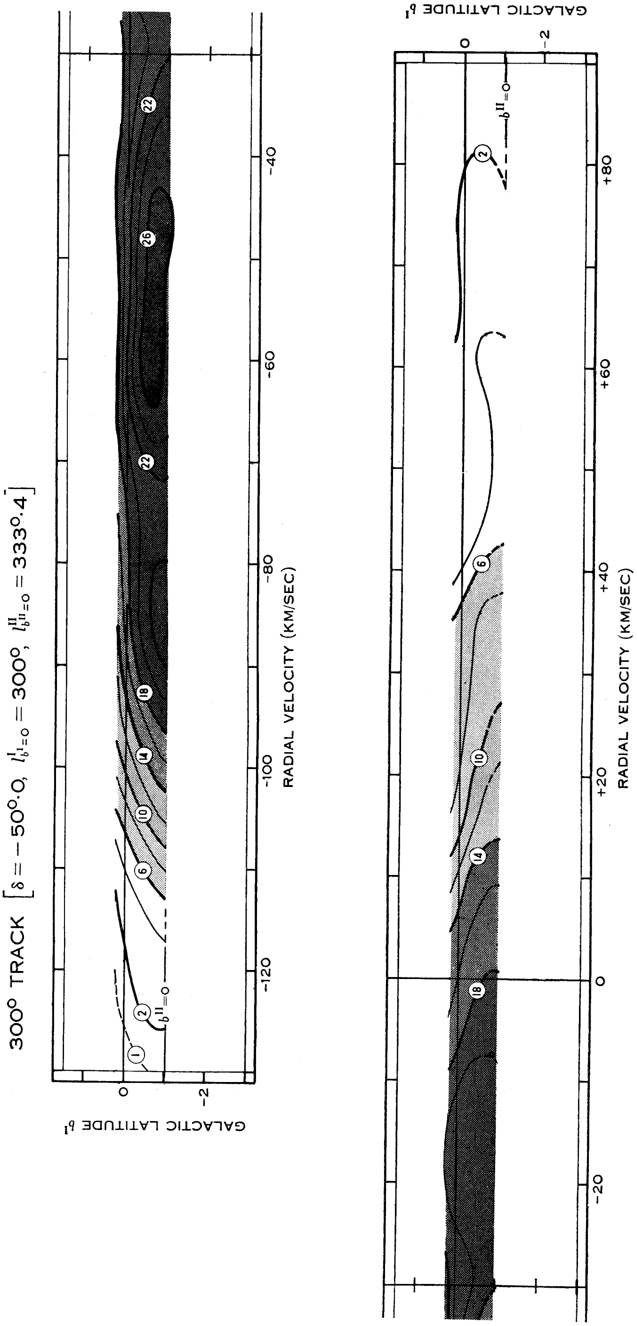

21 CM SURVEY OF THE SOUTHERN MILKY WAY

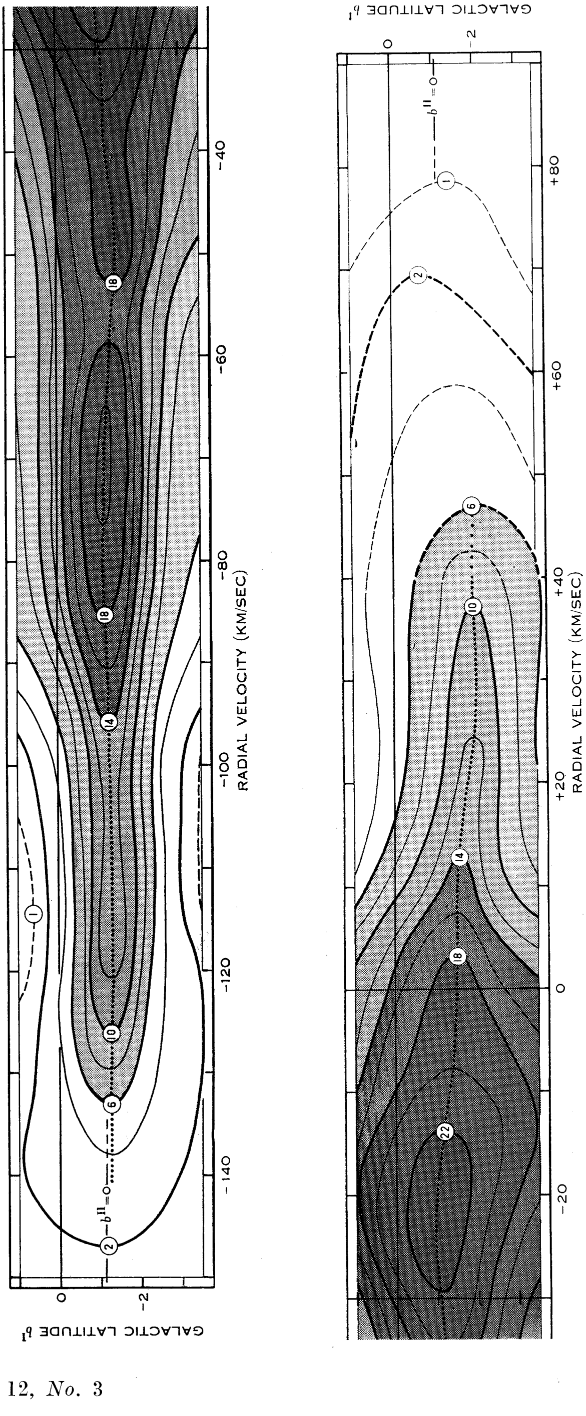

303°.6 TRACK $\left[\delta = -47°.4,\ l^{I}_{b^{I}=0} = 303°.6,\ l^{II}_{b^{II}=0} = 337°.0\right]$

21 CM SURVEY OF THE SOUTHERN MILKY WAY

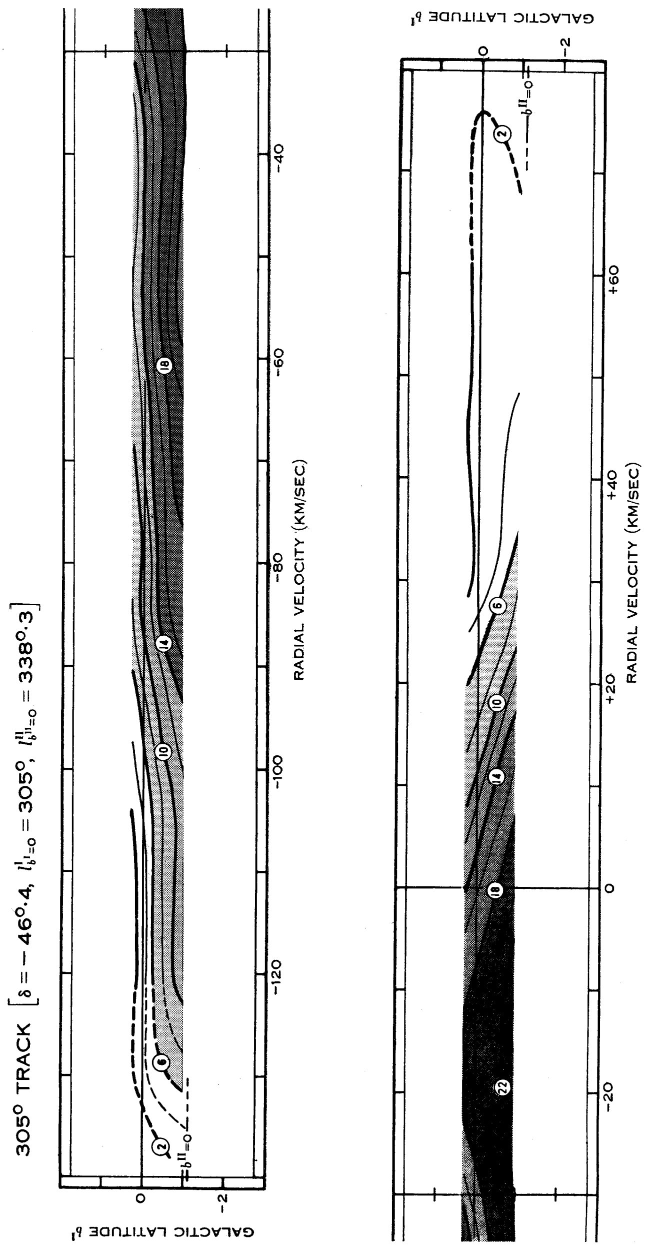

21 CM SURVEY OF THE SOUTHERN MILKY WAY

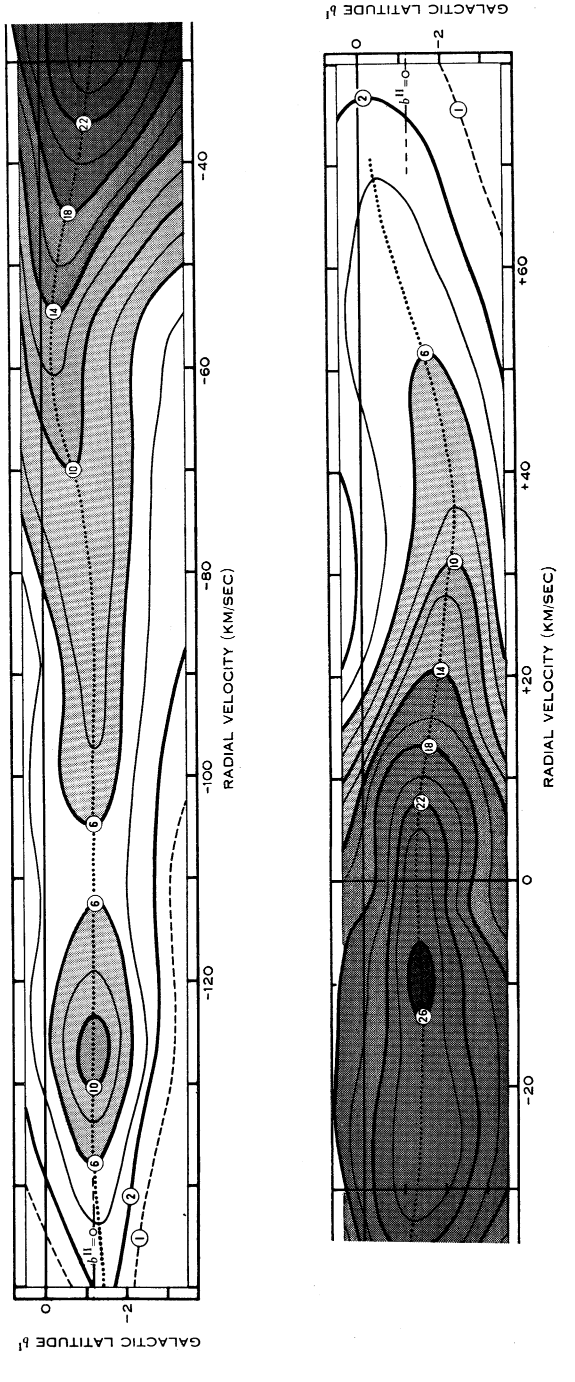

308°.8 TRACK $\left[\delta = -43°.6,\ l^I_{b^I=0} = 303°.8,\ l^{II}_{b^{II}=0} = 342°.1\right]$

21 CM SURVEY OF THE SOUTHERN MILKY WAY

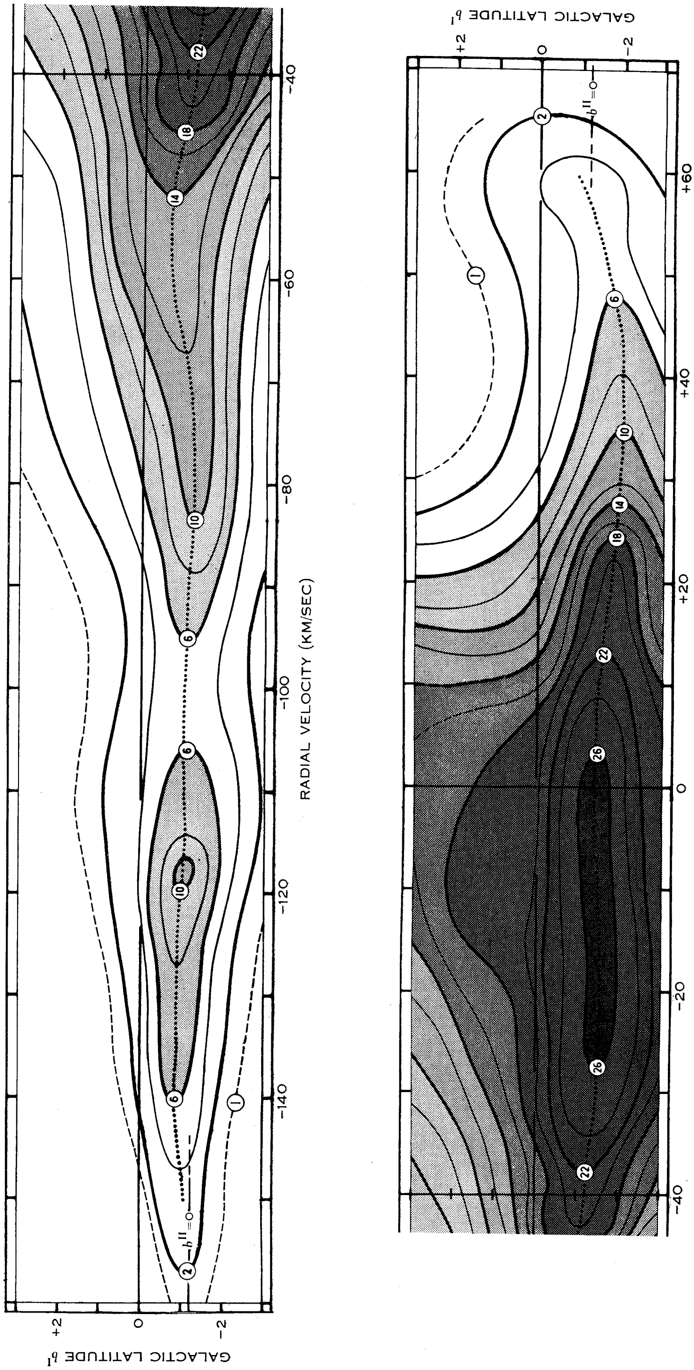

310° TRACK $[\delta = -42°\cdot 7,\ l^{I}_{b^{I}=0} = 310°,\ l^{II}_{b^{II}=0} = 343°\cdot 3]$

21 CM SURVEY OF THE SOUTHERN MILKY WAY

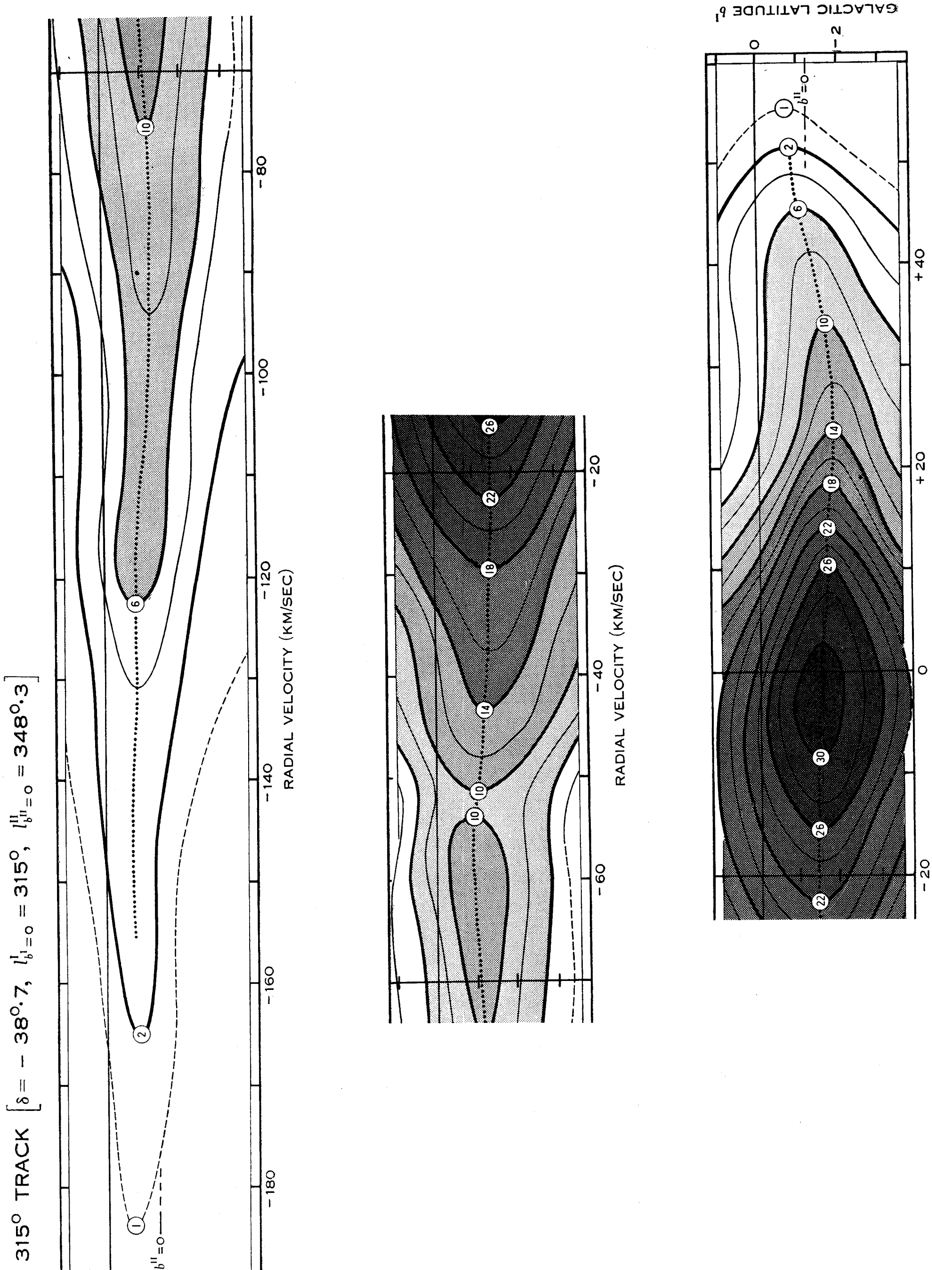

21 CM SURVEY OF THE SOUTHERN MILKY WAY

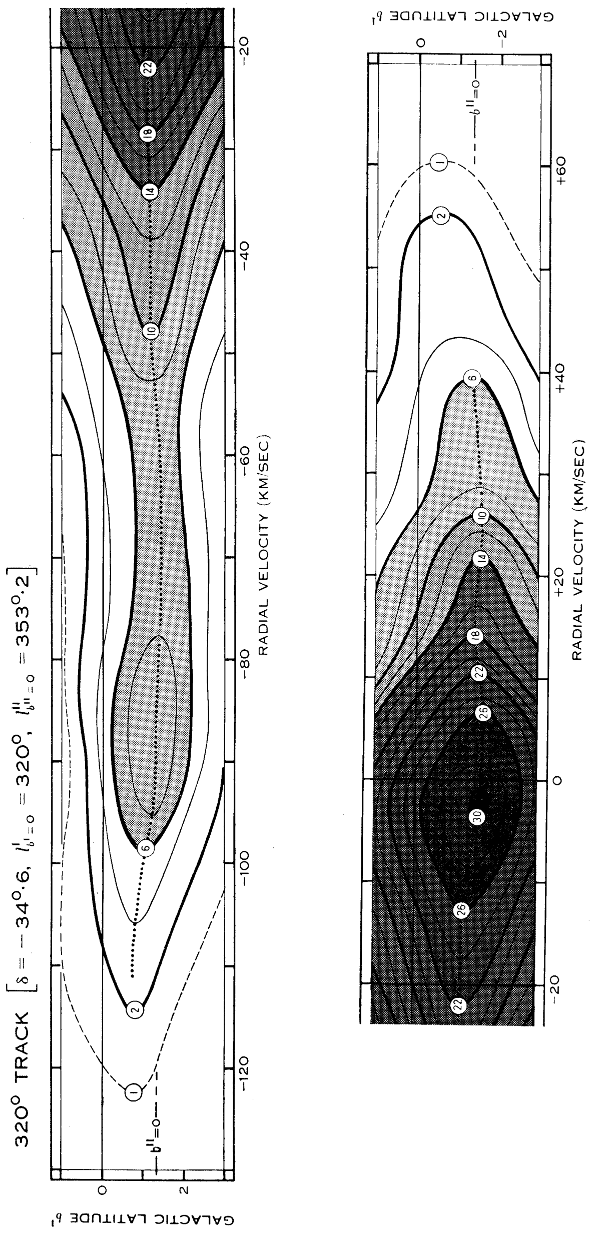

21 CM SURVEY OF THE SOUTHERN MILKY WAY

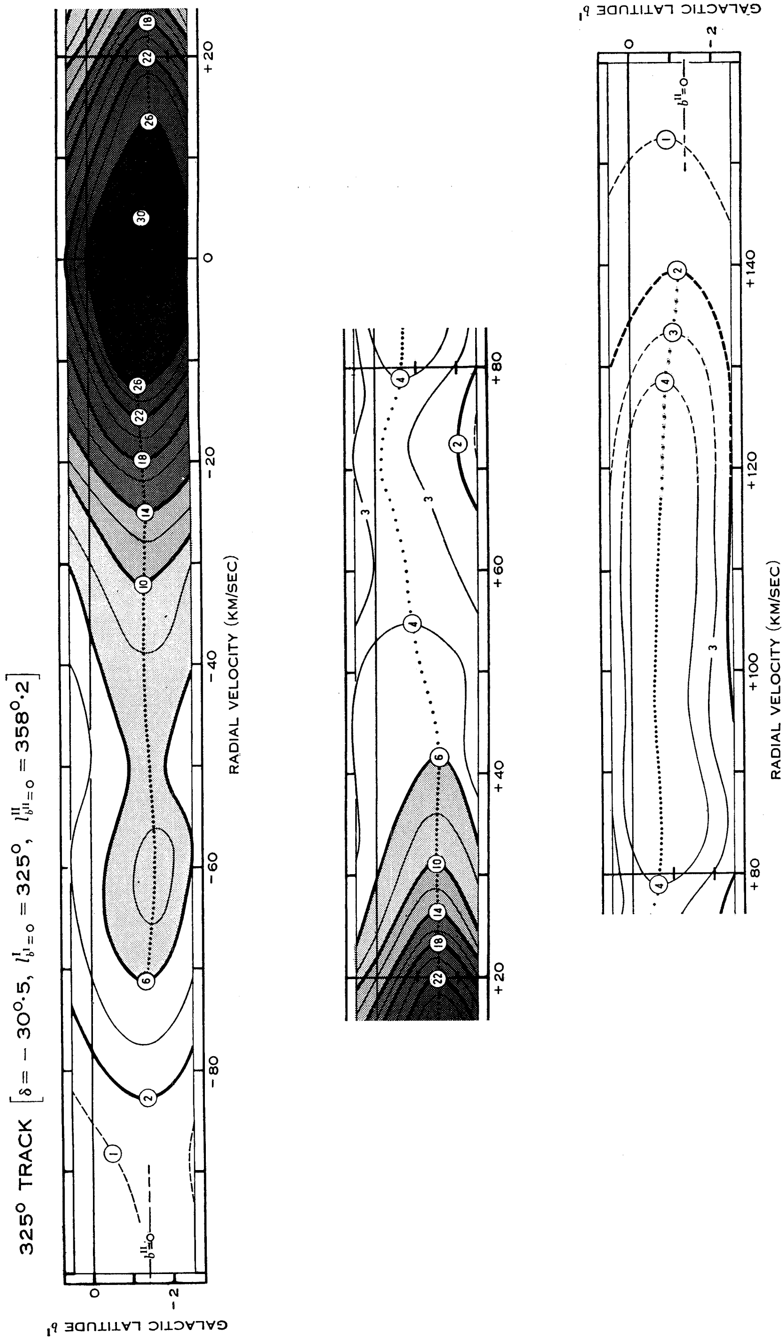

21 CM SURVEY OF THE SOUTHERN MILKY WAY

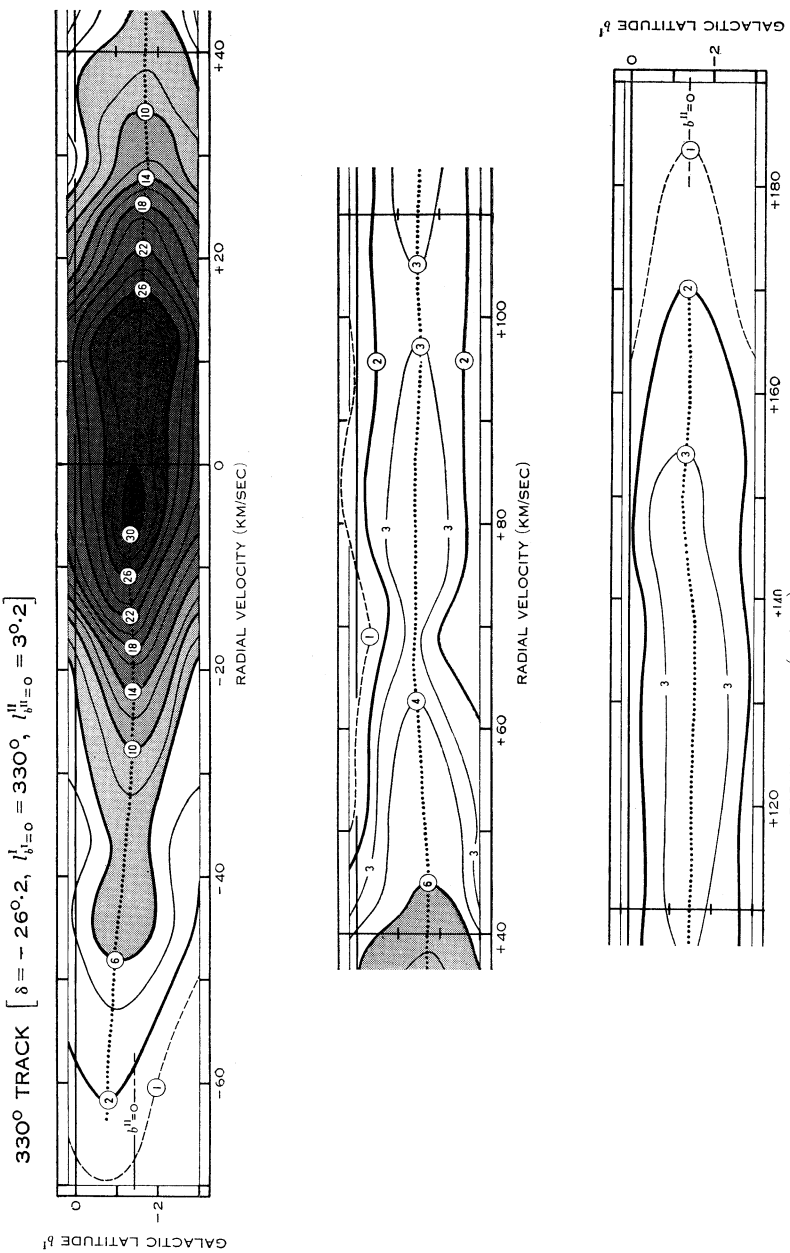

21 CM SURVEY OF THE SOUTHERN MILKY WAY

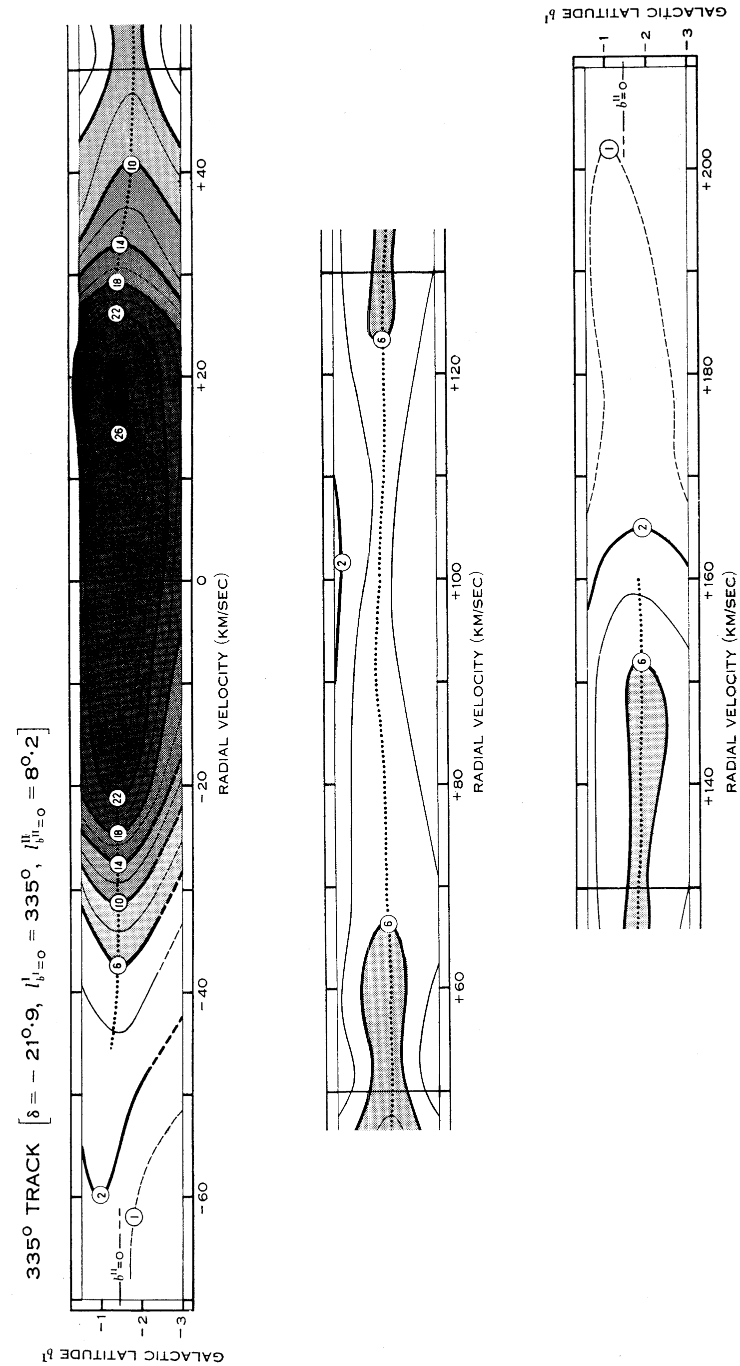

21 CM SURVEY OF THE SOUTHERN MILKY WAY

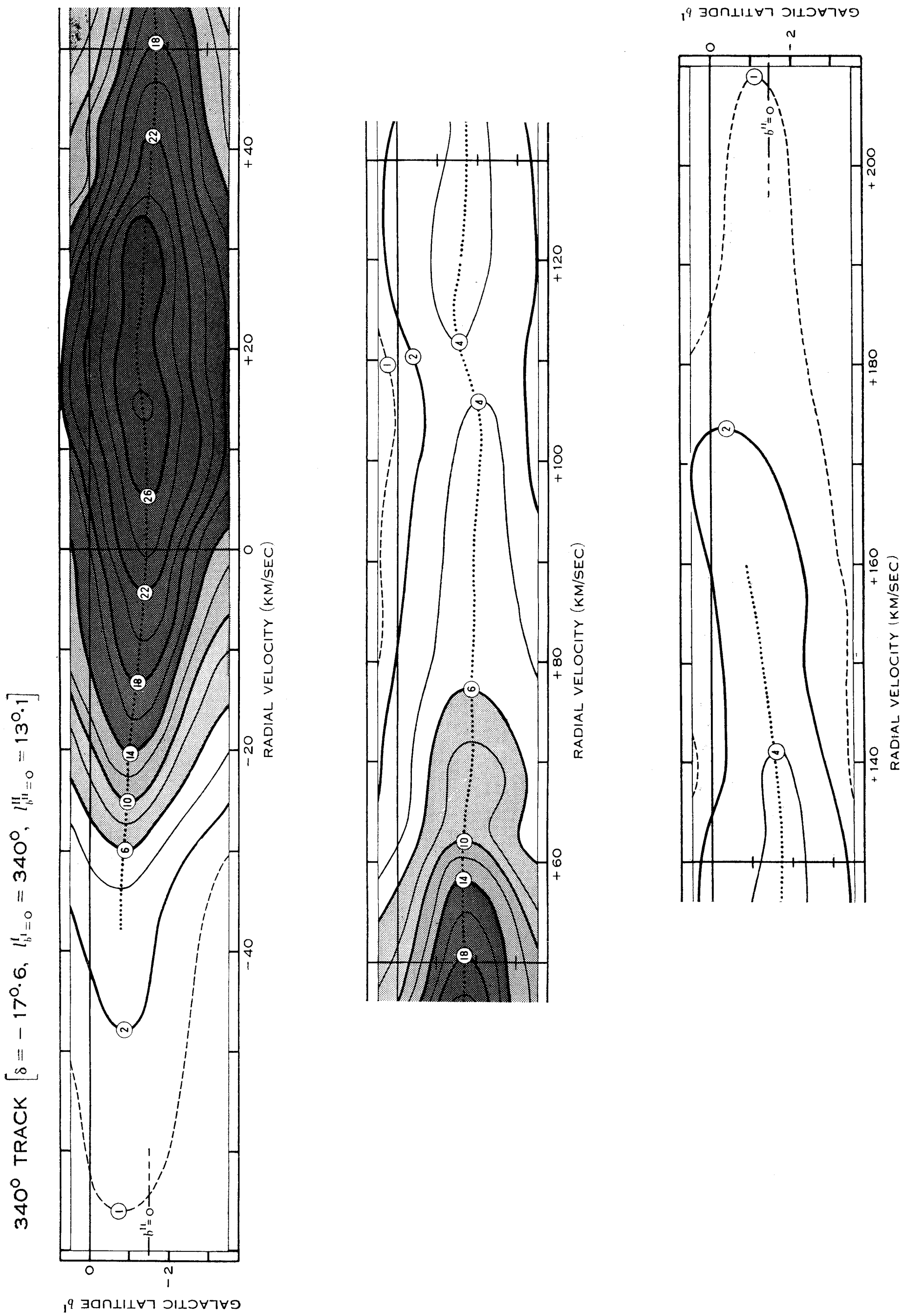

21 CM SURVEY OF THE SOUTHERN MILKY WAY

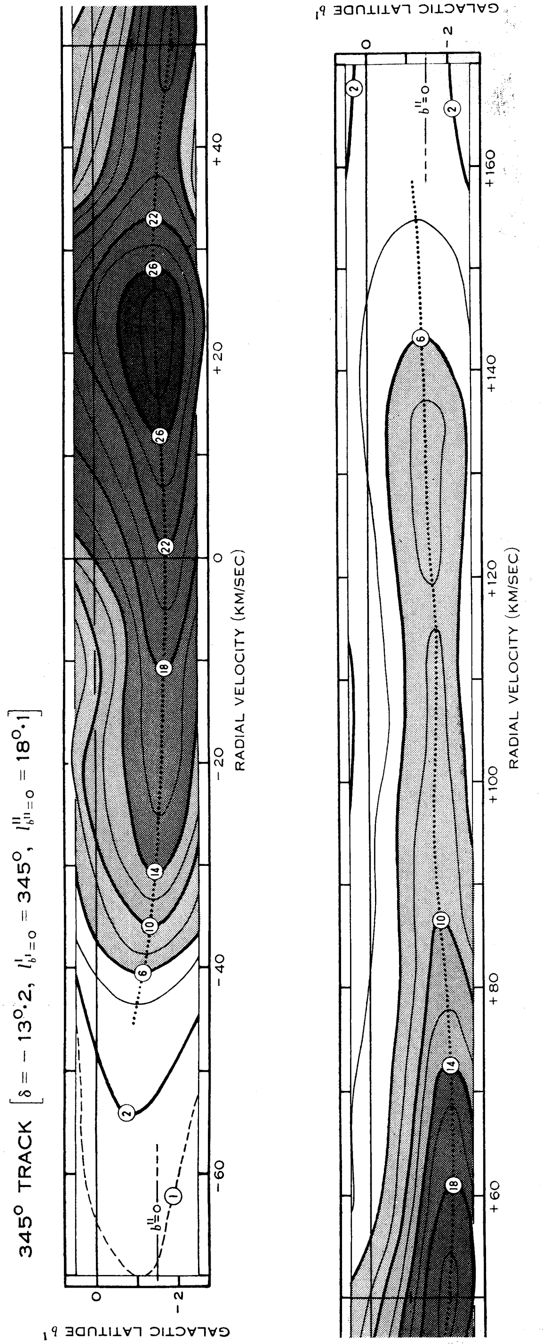

21 CM SURVEY OF THE SOUTHERN MILKY WAY

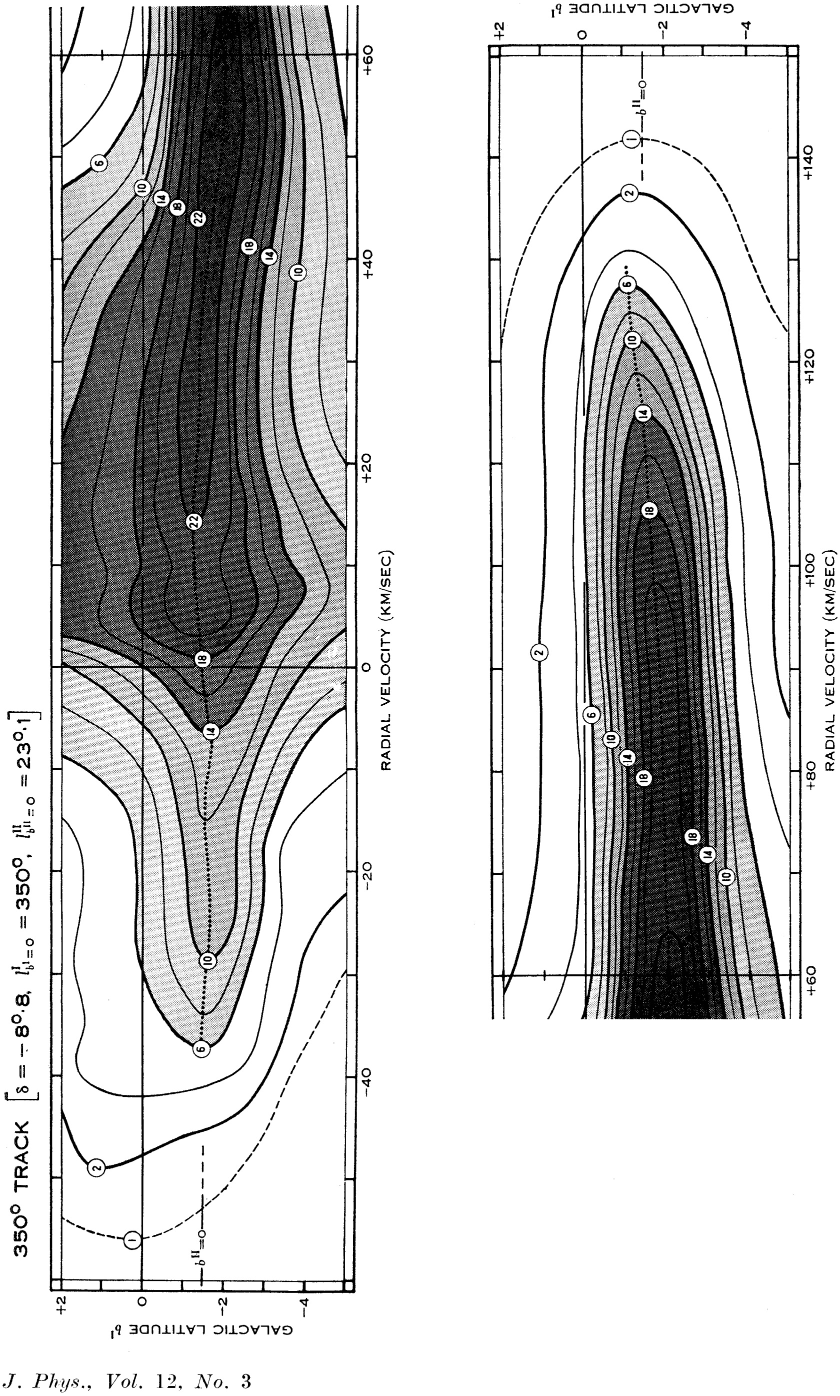

21 CM SURVEY OF THE SOUTHERN MILKY WAY

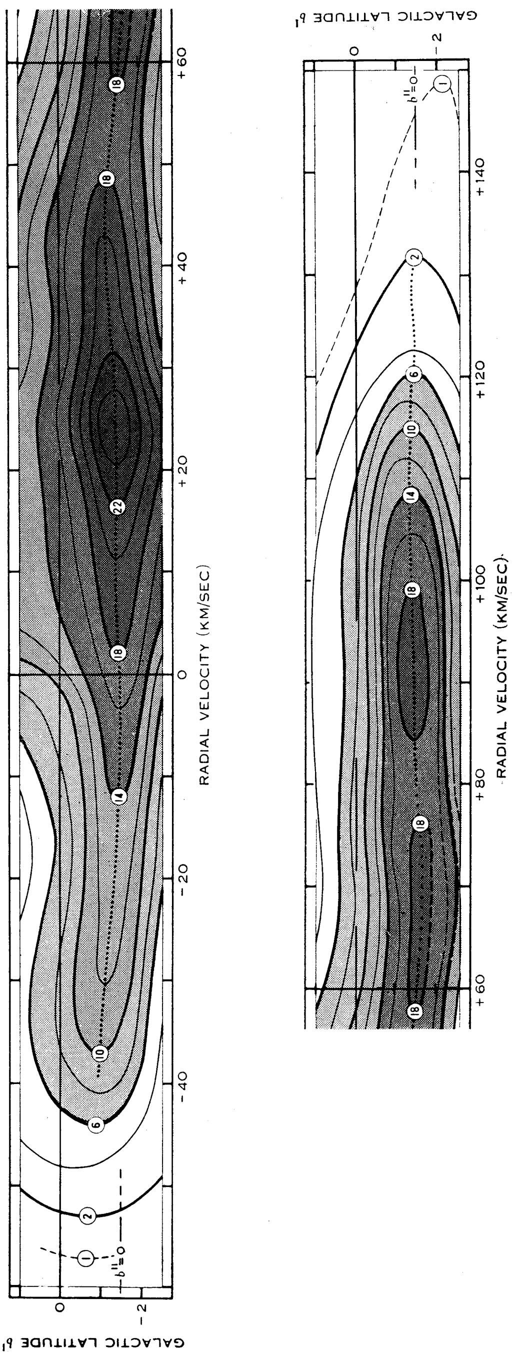

353°.4 TRACK $\left[\delta = -5°.8,\ l^I_{b^I=0} = 353°.4,\ l^{II}_{b^{II}=0} = 26°.5\right]$

21 CM SURVEY OF THE SOUTHERN MILKY WAY

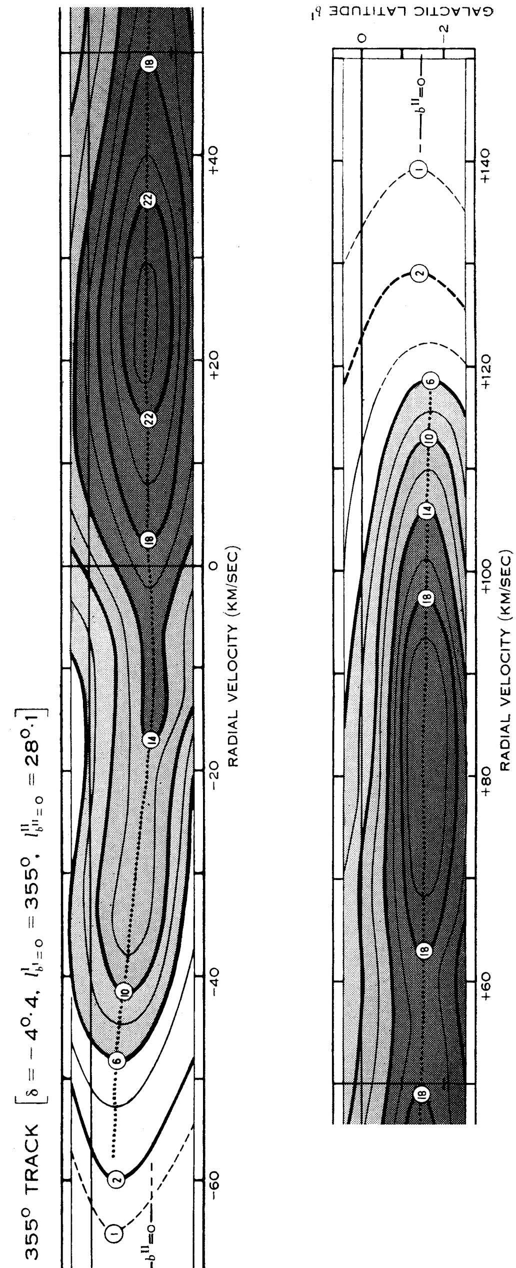

21 CM SURVEY OF THE SOUTHERN MILKY WAY

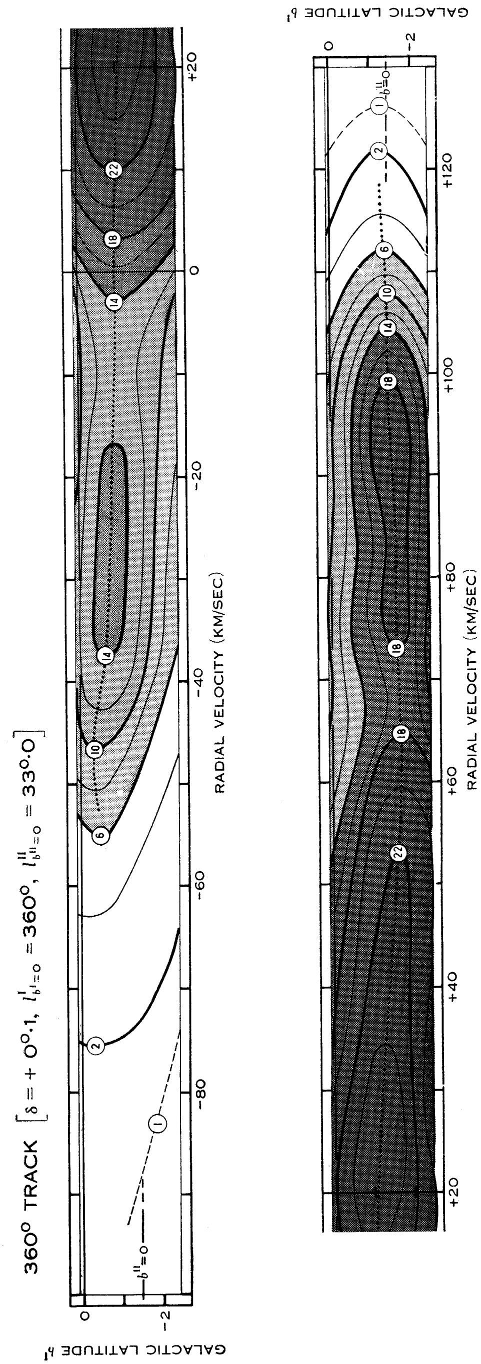

21 CM SURVEY OF THE SOUTHERN MILKY WAY

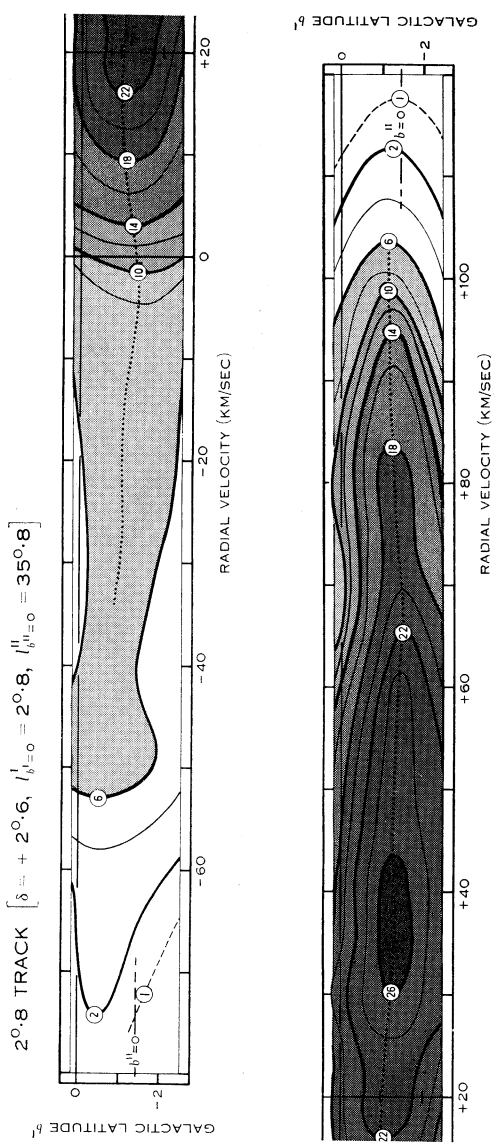

21 CM SURVEY OF THE SOUTHERN MILKY WAY

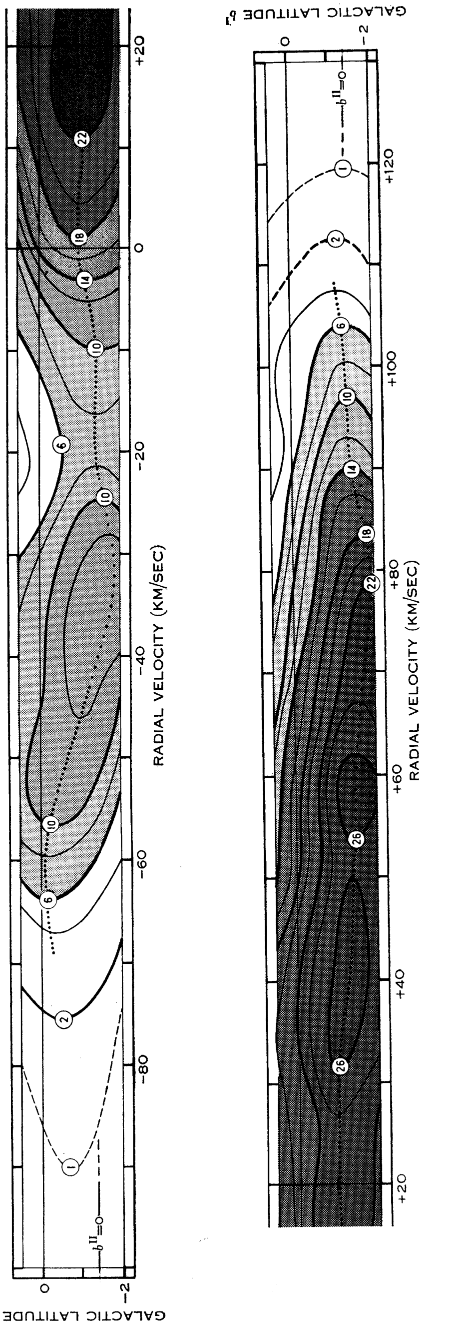

5° TRACK $\left[\delta = +4^\circ.5,\ l^I_{b^I=0} = 5^\circ,\ l^{II}_{b^{II}=0} = 38^\circ.0\right]$